Ti and Zr complexes bearing guanidine–phenolate ligands: coordination chemistry and polymerization studies

Víctor Flores-Romero, Jesse LeBlanc, Zichuan Chen and Gino G. Lavoie*

York University, Department of Chemistry

Toronto, Canada

Electronic Supporting Information

Table of Contents

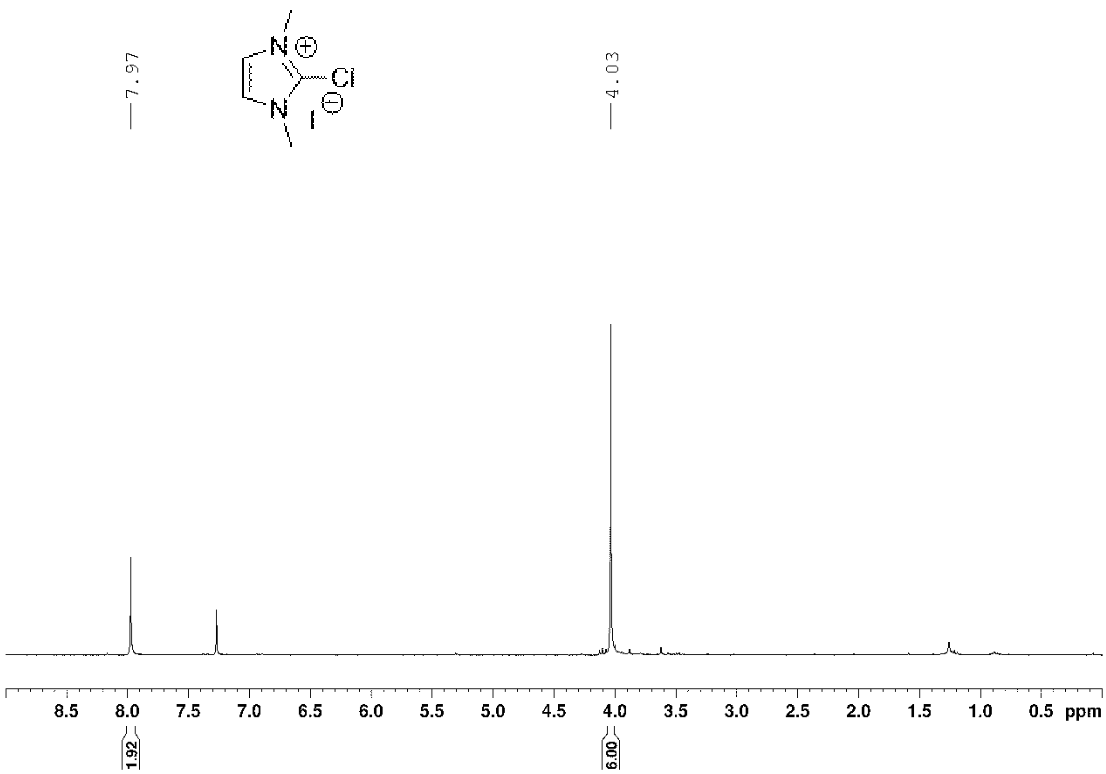

Figure S1. ^{1}H NMR spectrum of 1Cl (400 MHz, $CDCl_3$)

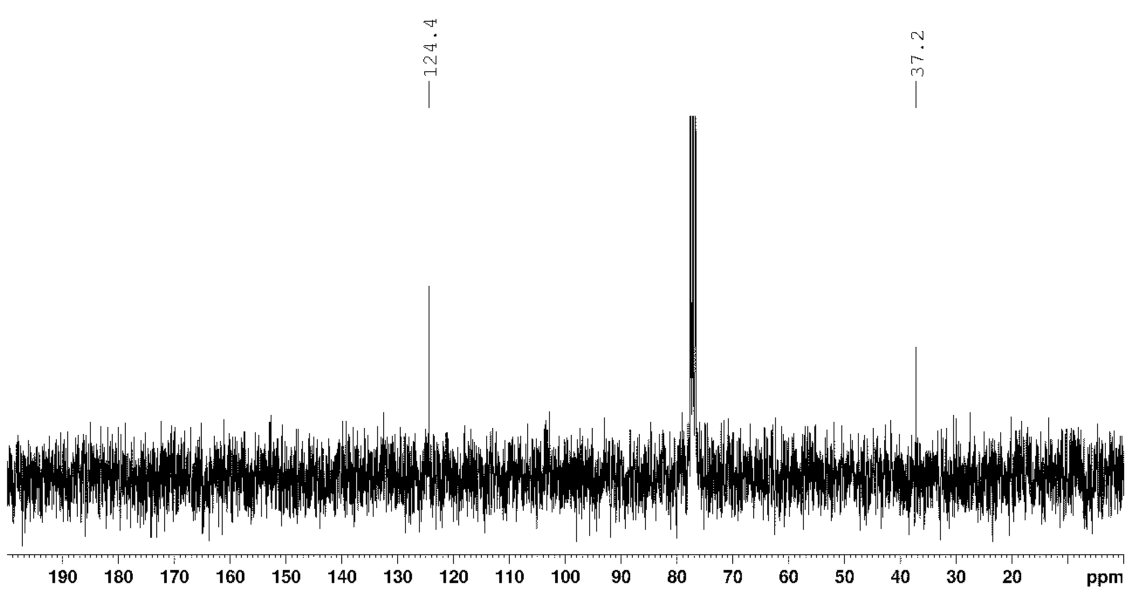

Figure S2. $^{13}C\{^{1}H\}$ NMR spectrum of 1Cl (100 MHz, $CDCl_3$)

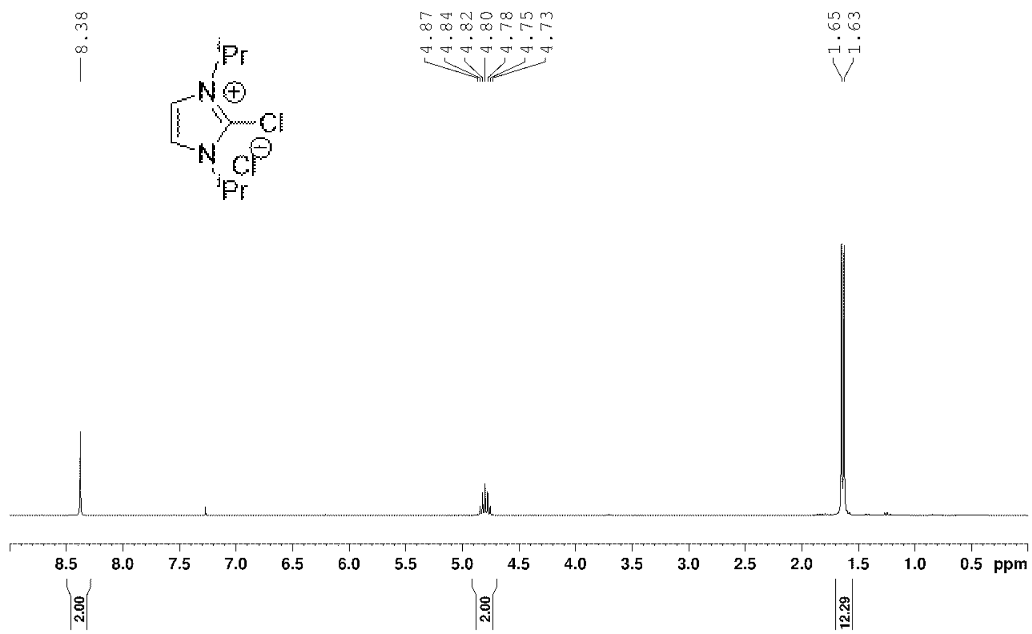

Figure S3. ^{1}H NMR spectrum of 2Cl (300 MHz, $CDCl_3$)

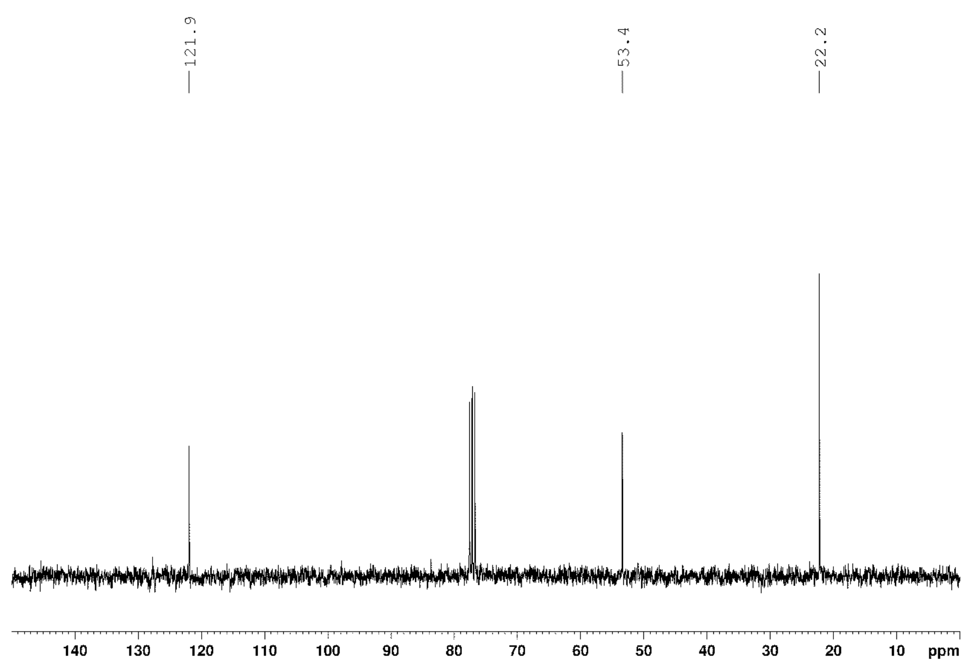

Figure S4. $^{13}C\{^{1}H\}$ NMR spectrum of 2Cl (100 MHz, $CDCl_3$)

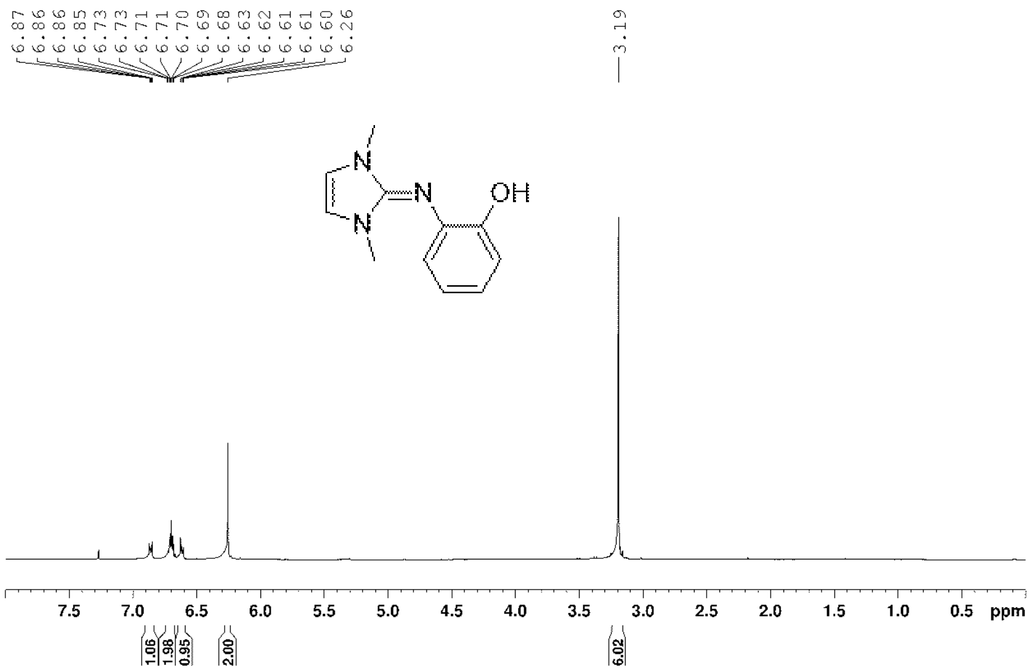

Figure S5. ^{1}H NMR spectrum of L1H (300 MHz, $CDCl_3$)

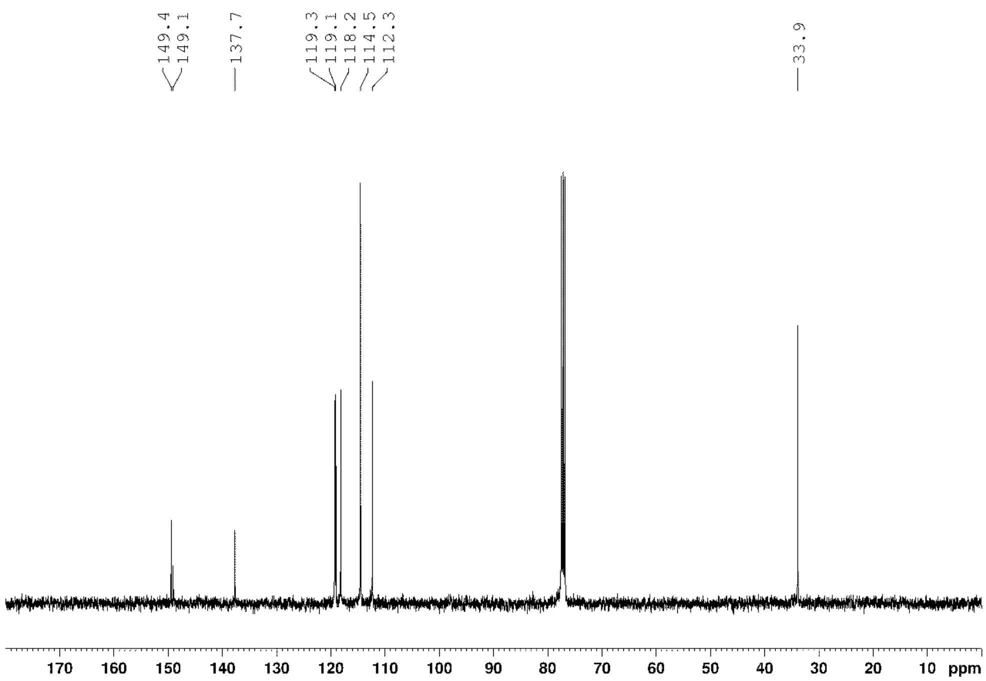

Figure S6. $^{13}C\{^{1}H\}$ NMR spectrum of L1H (75 MHz, $CDCl_3$)

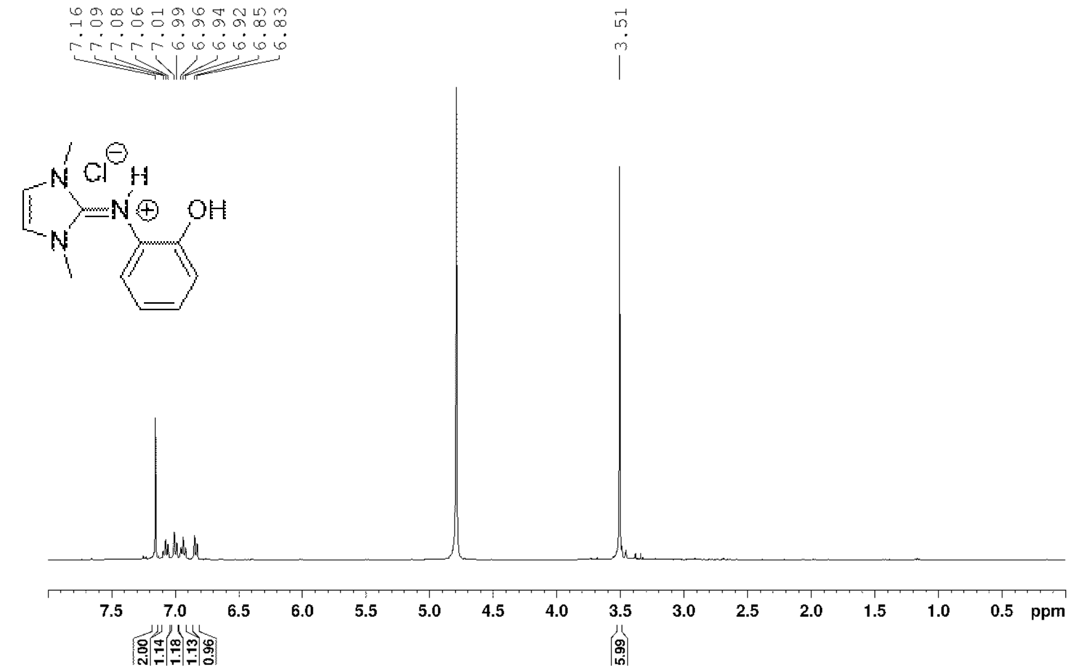

Figure S7. [1]H NMR spectrum of L1H·HCl (400 MHz, D_2O)

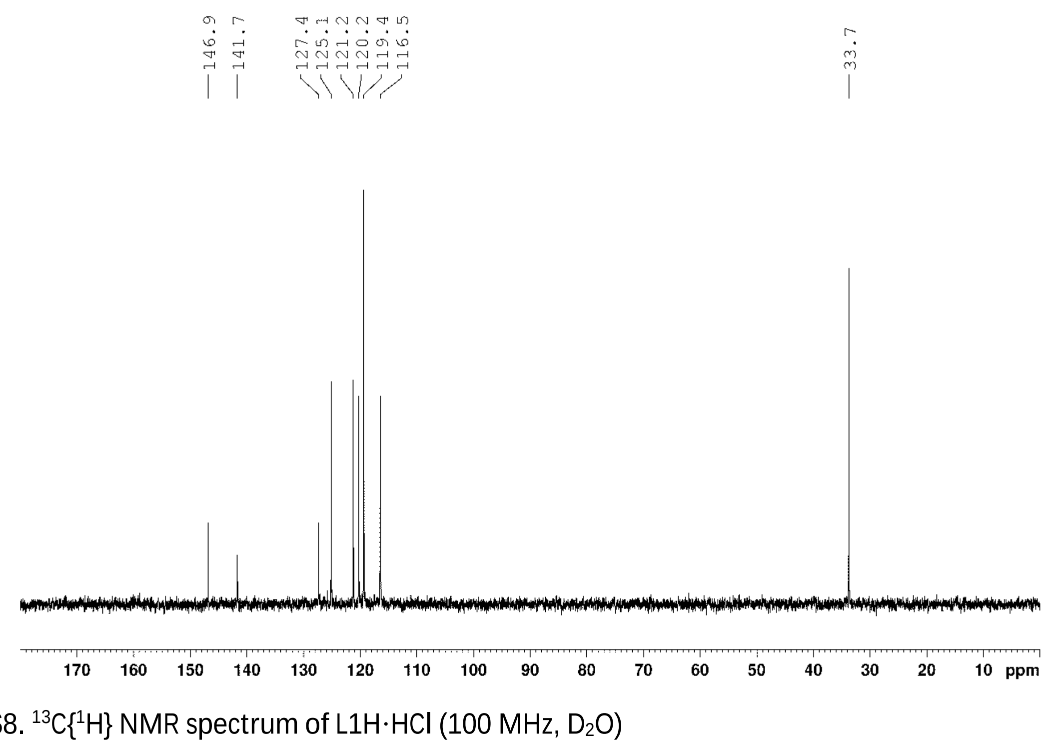

Figure S8. [13]C{[1]H} NMR spectrum of L1H·HCl (100 MHz, D_2O)

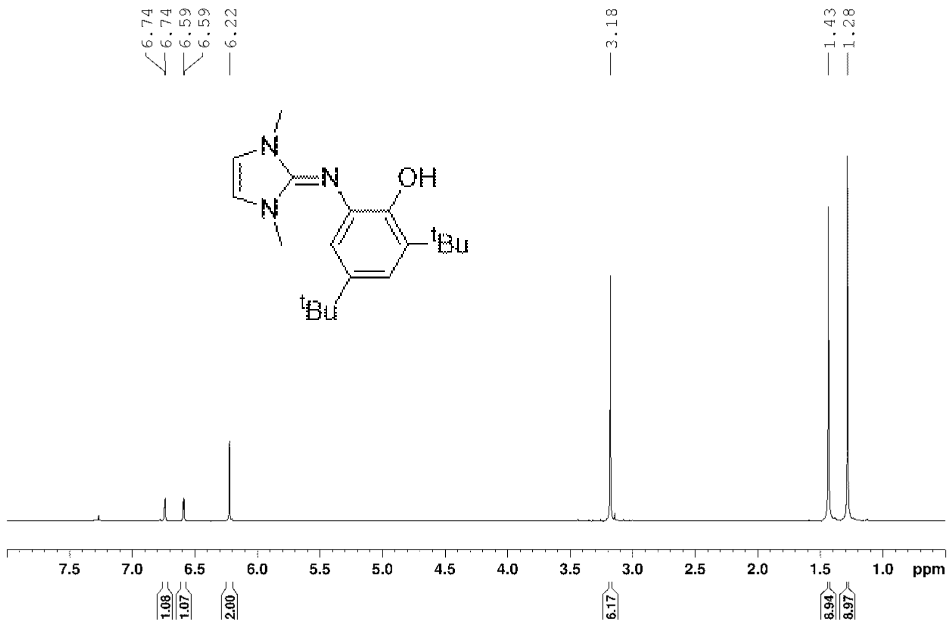

Figure S9. ^{1}H NMR spectrum of L1'H (400 MHz, $CDCl_3$)

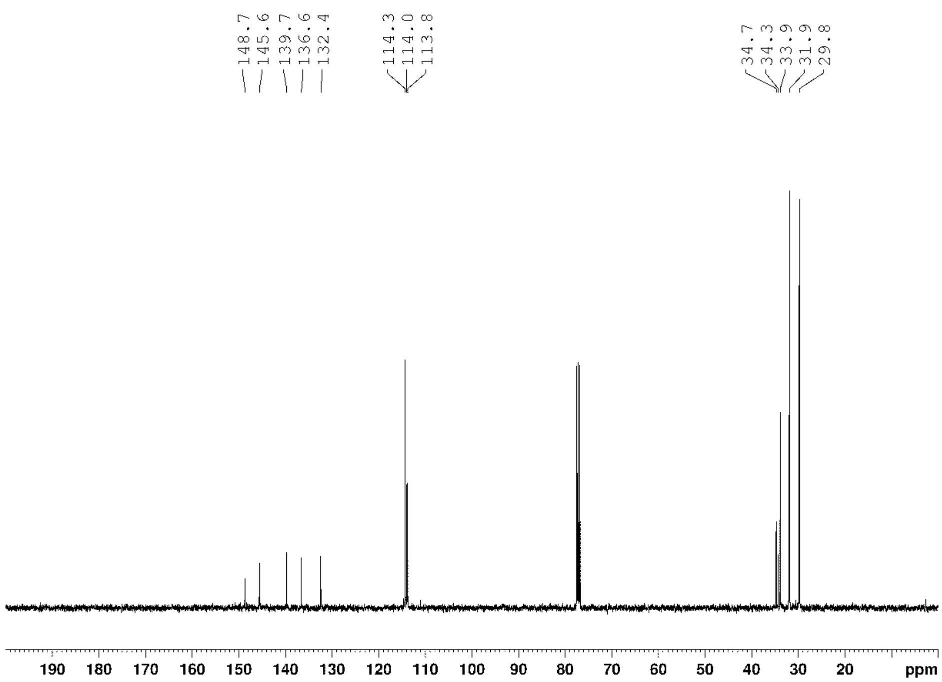

Figure S10. $^{13}C\{^{1}H\}$ NMR spectrum of L1'H (75 MHz, $CDCl_3$)

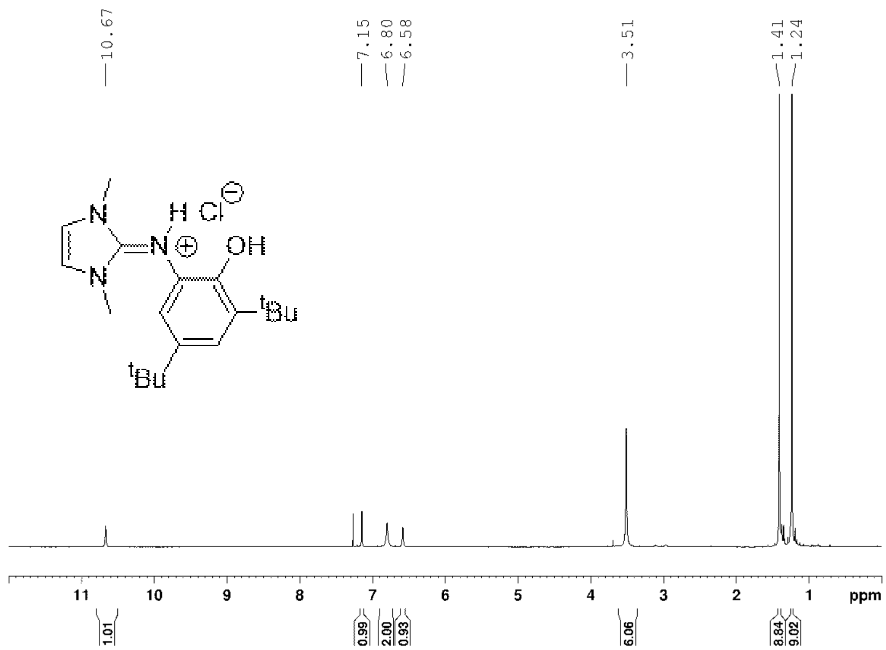

Figure S11. ^{1}H NMR spectrum of L1'H·HCl (400 MHz, $CDCl_3$)

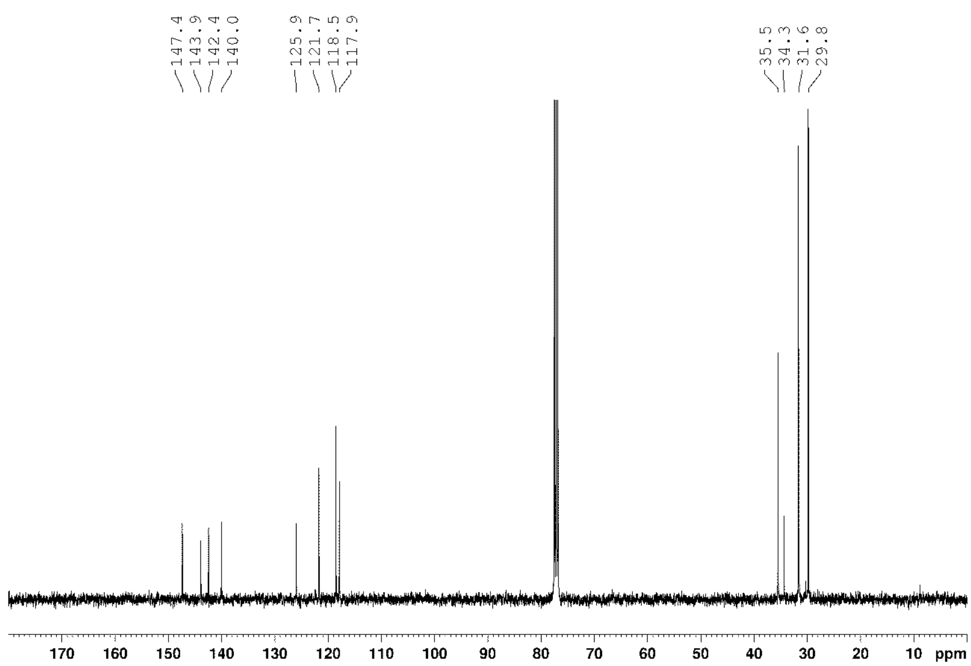

Figure S12. ^{13}C NMR spectrum of L1'H·HCl (100 MHz, $CDCl_3$)

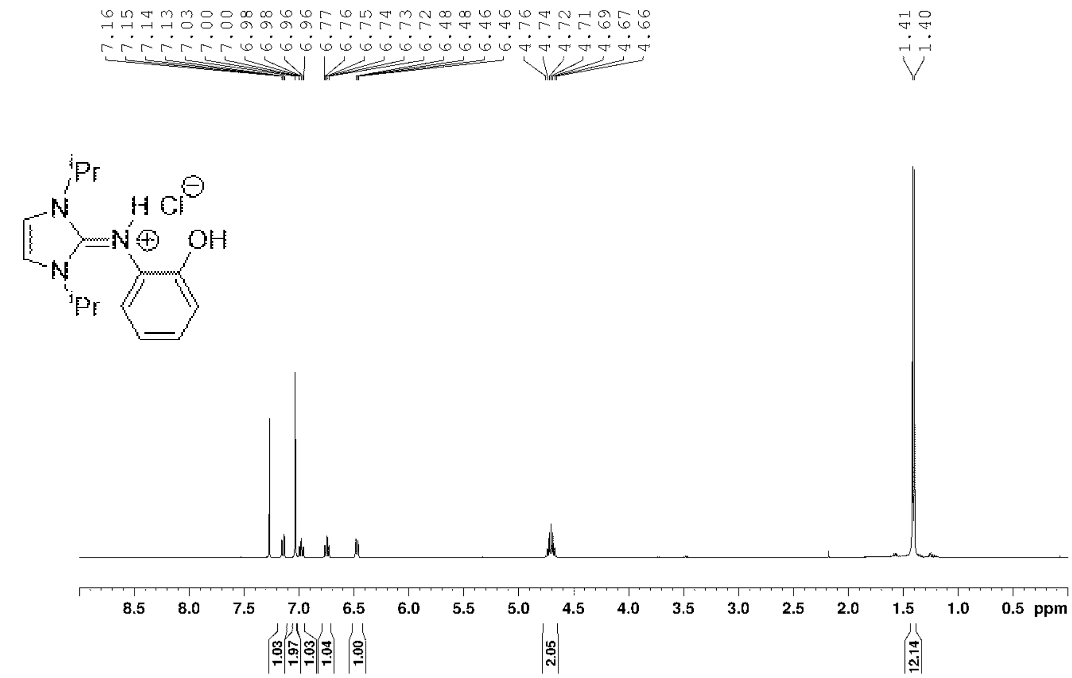

Figure S13. ^{1}H NMR spectrum of L2H·HCl (300 MHz, $CDCl_3$)

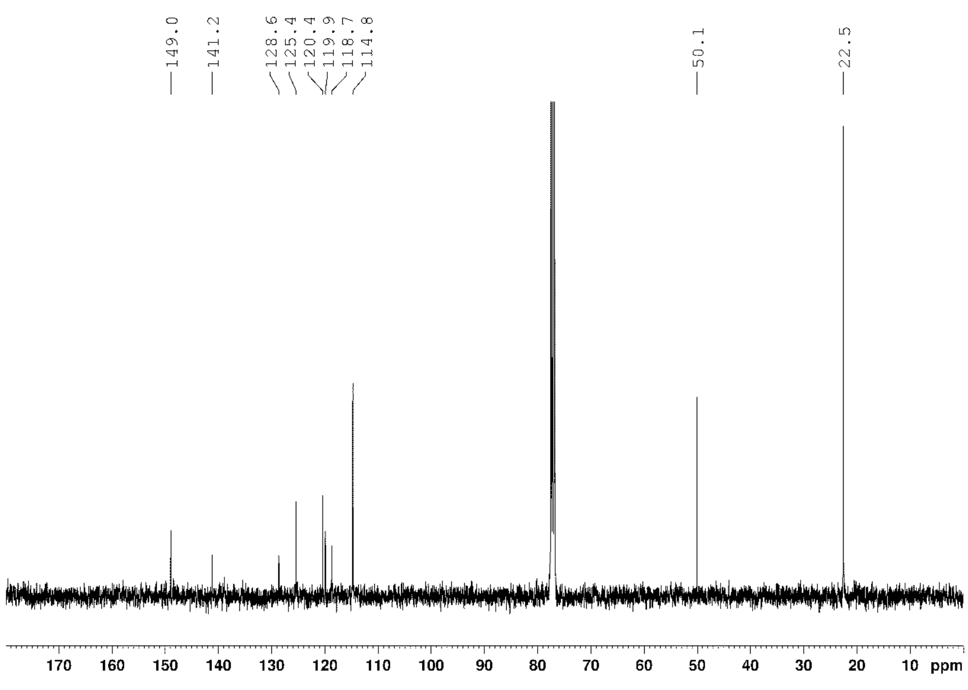

Figure S14. $^{13}C\{^{1}H\}$ NMR spectrum of L2H·HCl (75 MHz, $CDCl_3$)

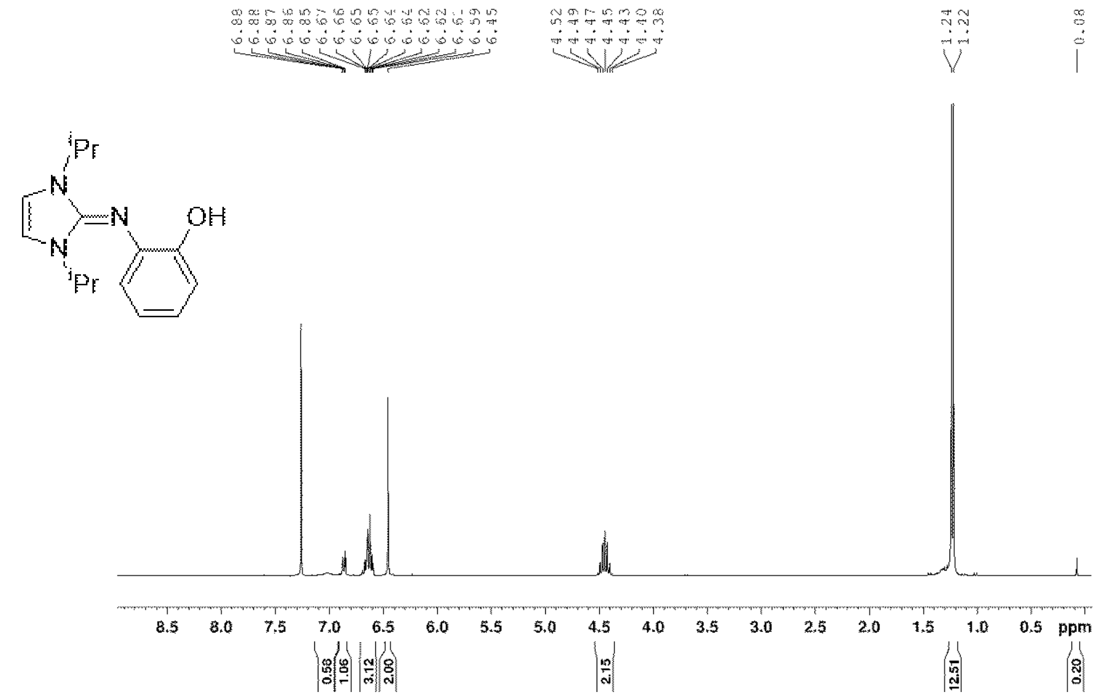

Figure S15. ^{1}H NMR spectrum of L2H (300 MHz, $CDCl_3$)

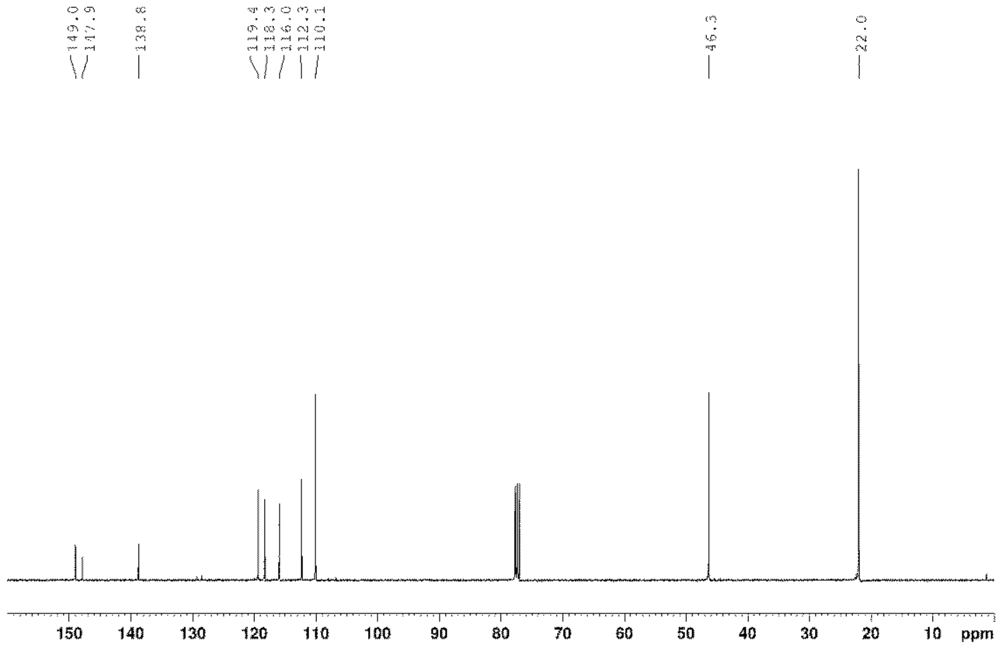

Figure S16. $^{13}C\{^{1}H\}$ NMR spectrum of L2H (75 MHz, $CDCl_3$)

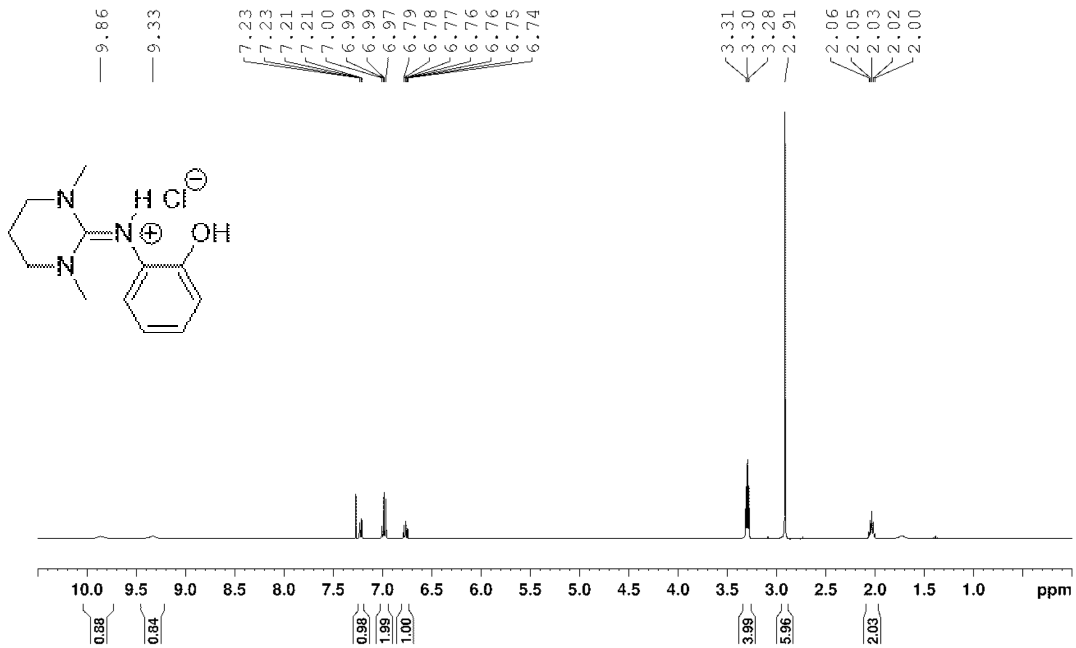

Figure S17. ^{1}H NMR spectrum of L4H·HCl (400 MHz, $CDCl_3$)

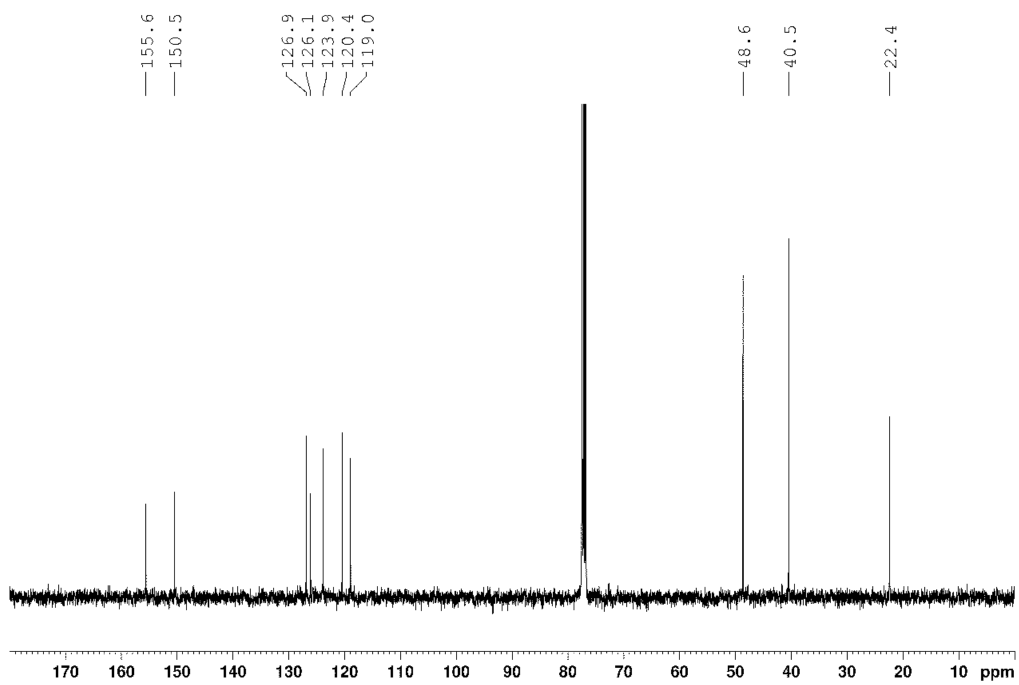

Figure S18. $^{13}C\{^{1}H\}$ NMR spectrum of L4H·HCl (100 MHz, $CDCl_3$)

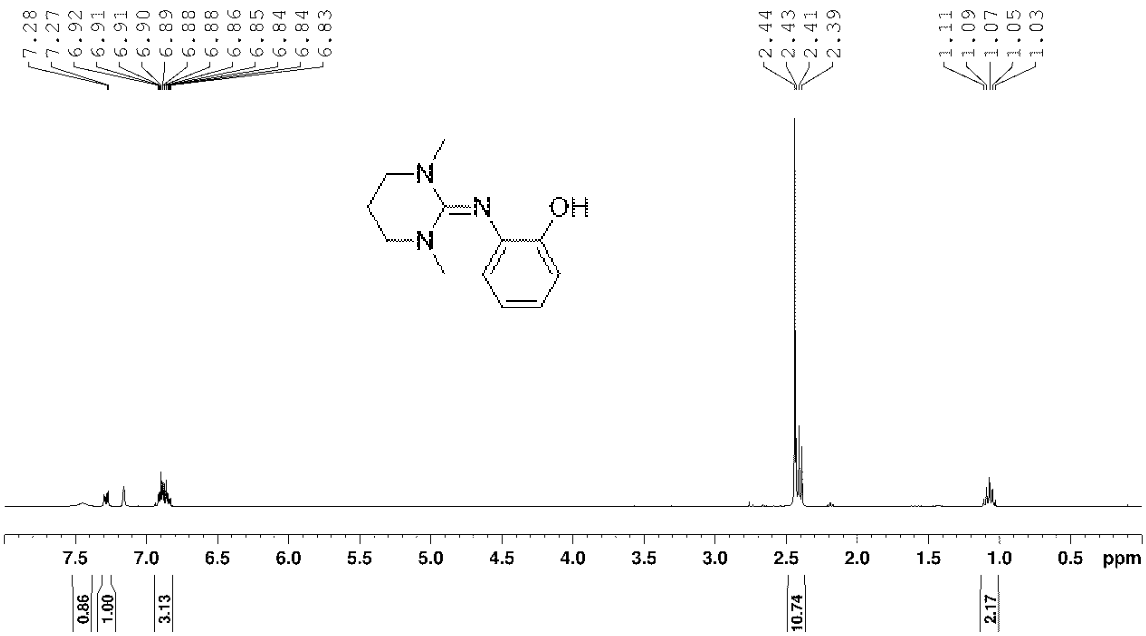

Figure S19. ^{1}H NMR spectrum of L4H (400 MHz, C_6D_6)

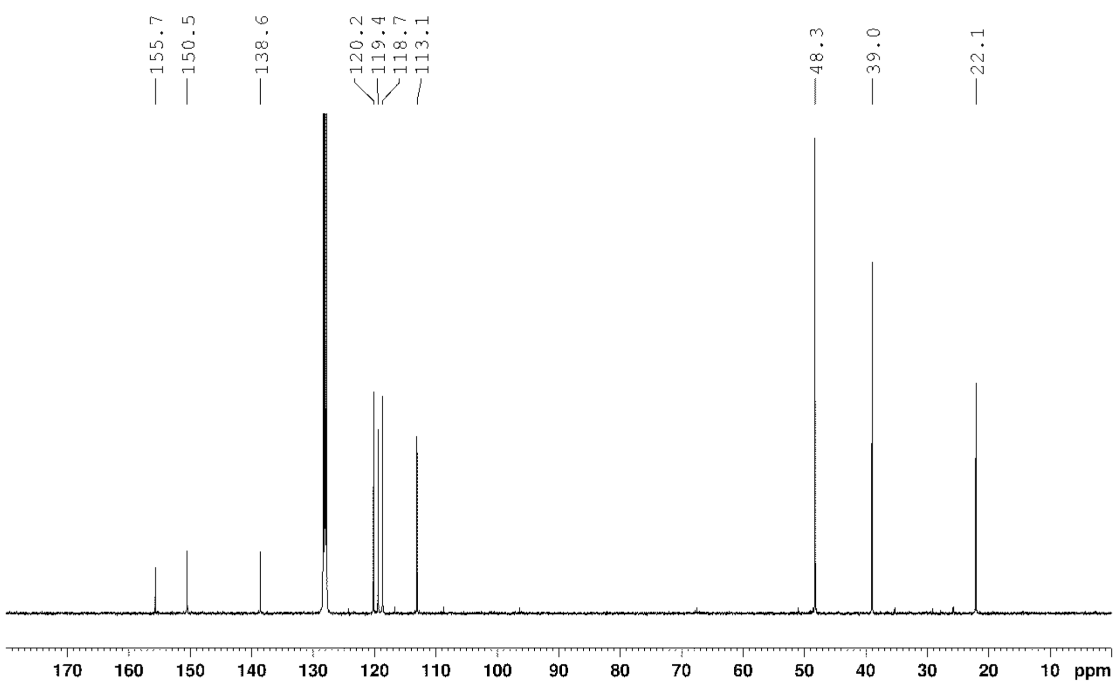

Figure S20. $^{13}C\{^{1}H\}$ NMR spectrum of L4H (100 MHz, C_6D_6)

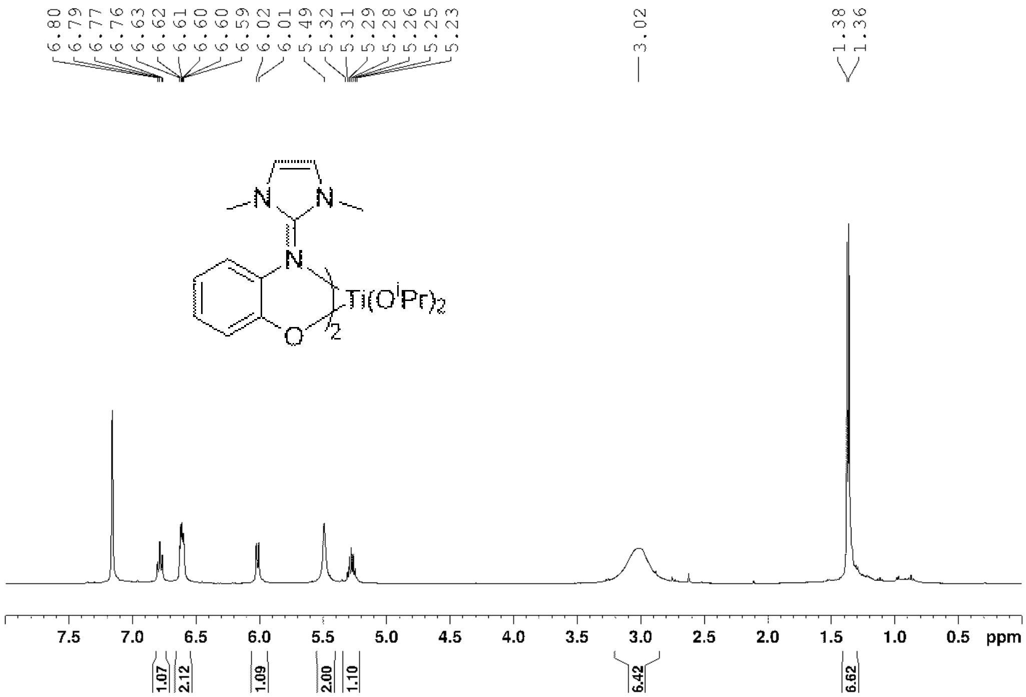

Figure S21. ^{1}H NMR spectrum of Ti1a (400 MHz, C_6D_6)

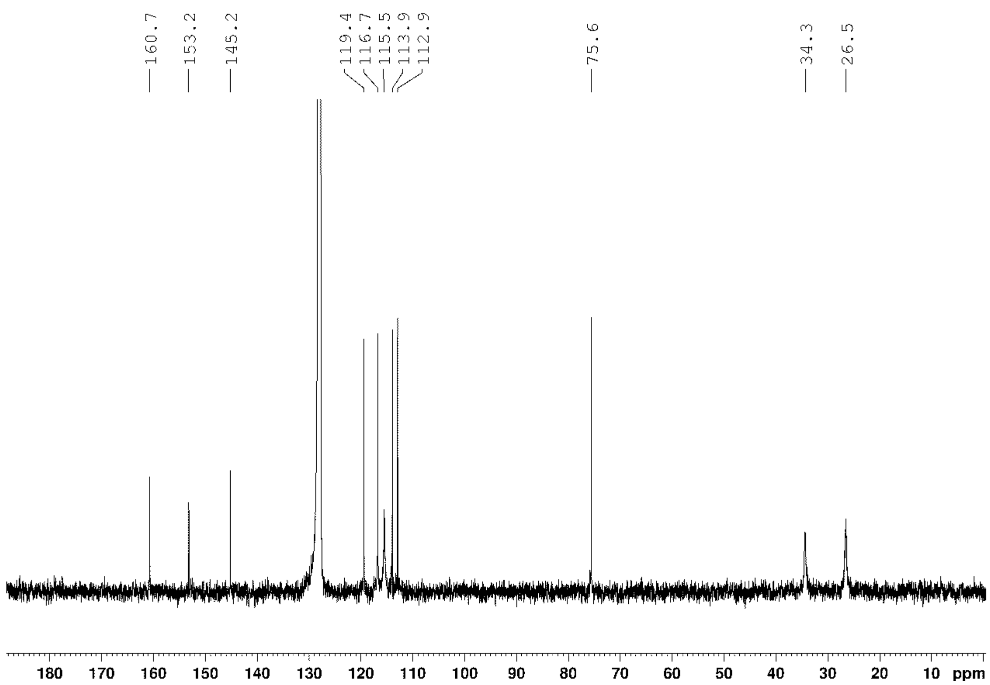

Figure S22. $^{13}C\{^{1}H\}$ NMR spectrum of Ti1a (100 MHz, C_6D_6)

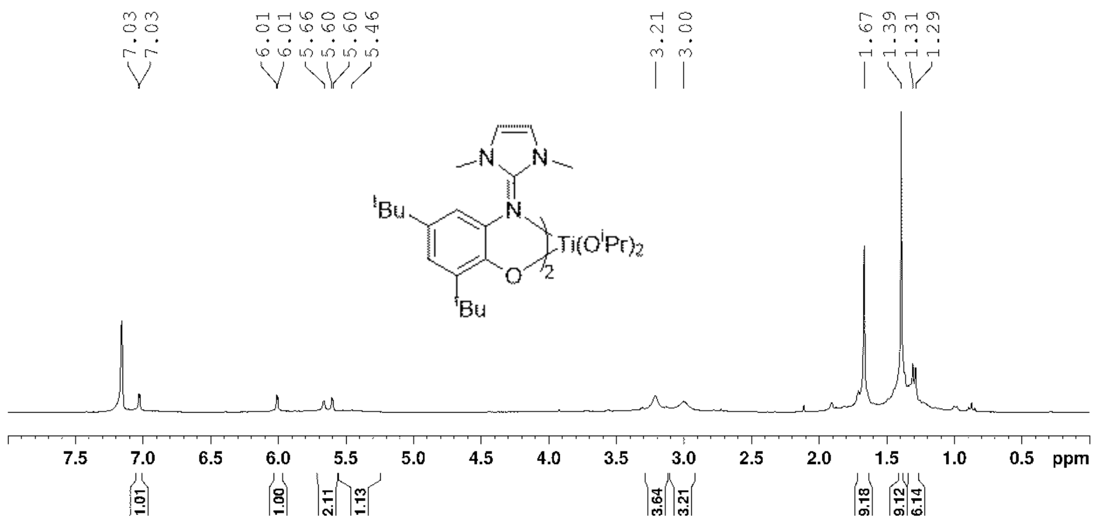

Figure S23.[1]H NMR spectrum of Ti1′a (400 MHz, C_6D_6)

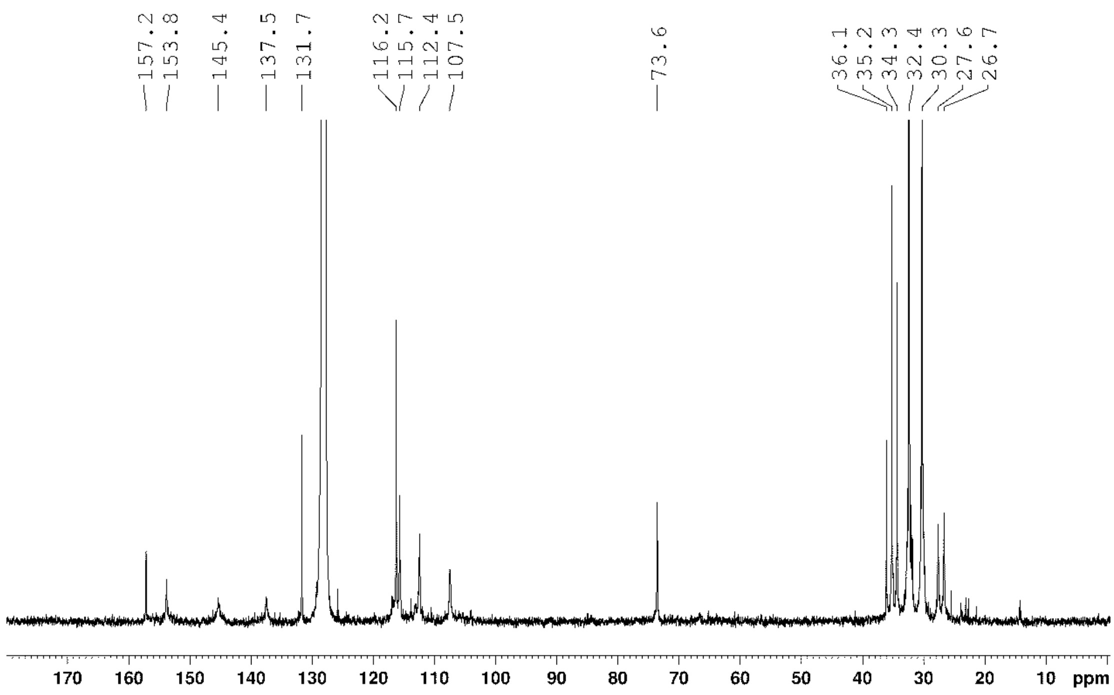

Figure S24.[13]C{[1]H} NMR spectrum of Ti1′a (100 MHz, C_6D_6)

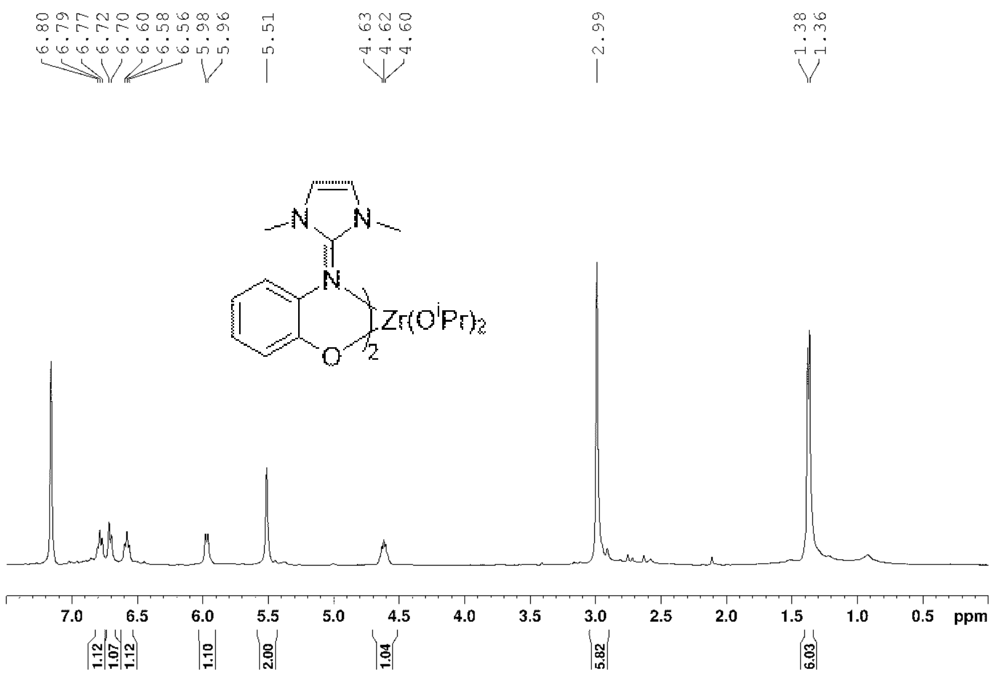

Figure S25. ^{1}H NMR spectrum of Zr1a (400 MHz, C_6D_6)

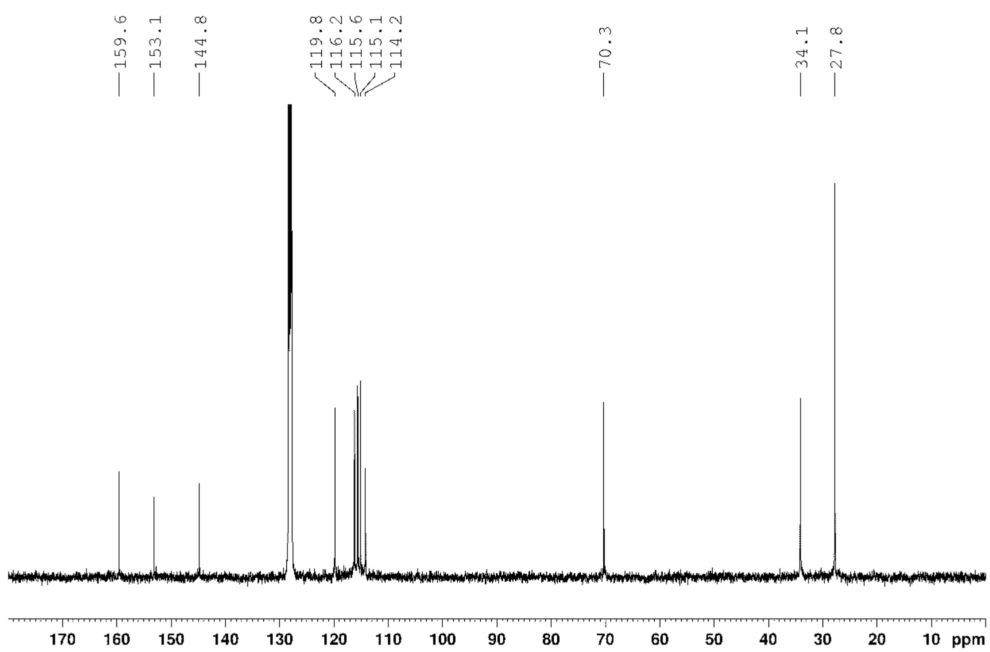

Figure S26. $^{13}C\{^{1}H\}$ NMR spectrum of Zr1a (100 MHz, C_6D_6)

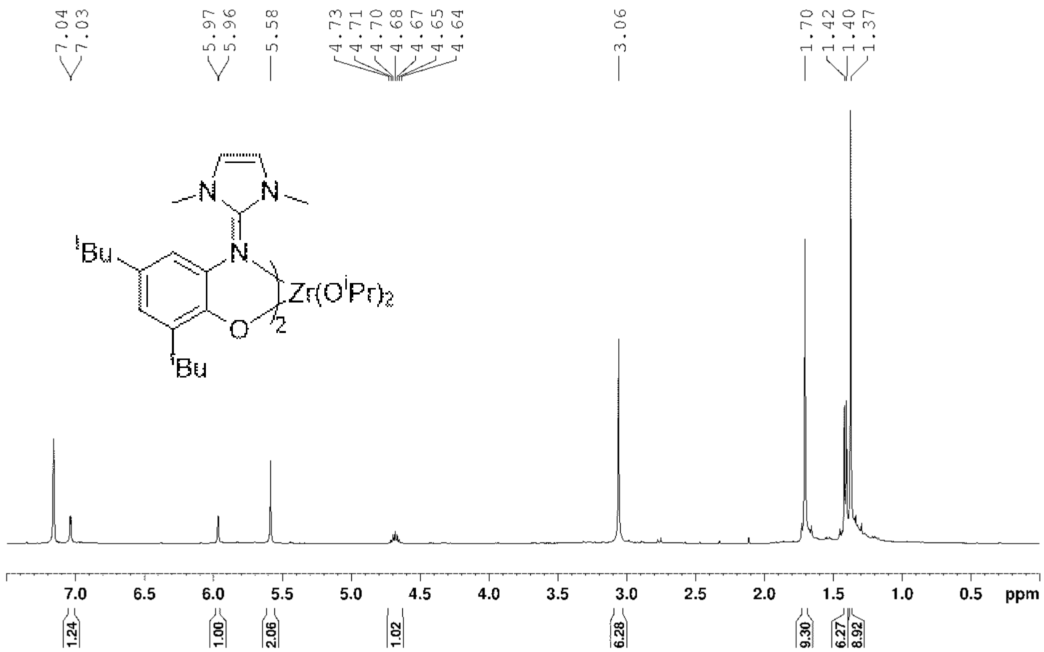

Figure S27.[1]H NMR spectrum of Zr1′a (400 MHz, C_6D_6)

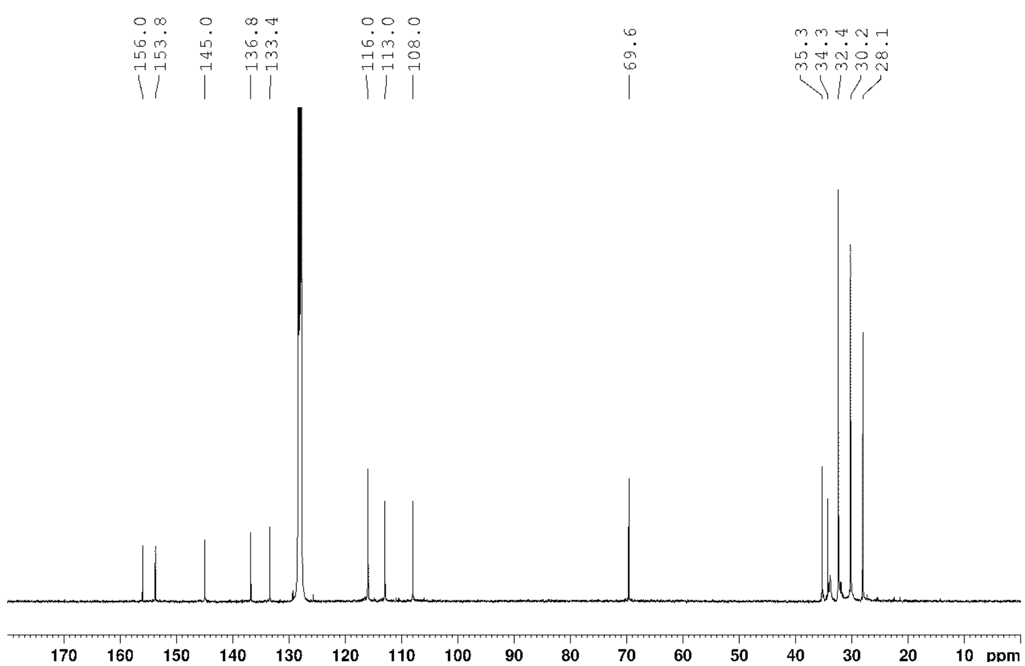

Figure S28.[13]C{[1]H} NMR spectrum of Zr1′a (100 MHz, C_6D_6)

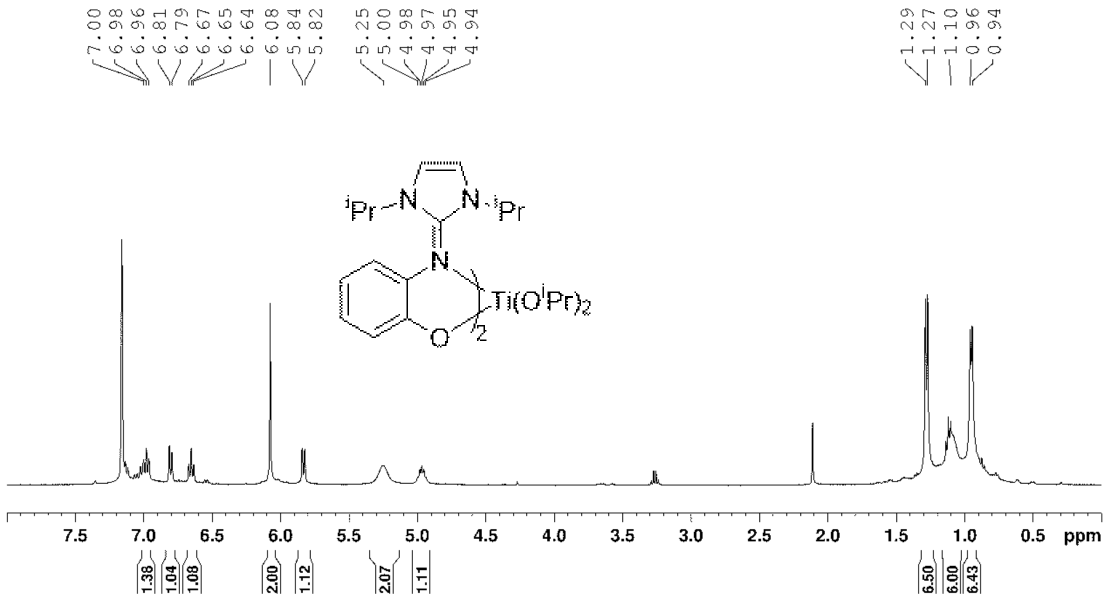

Figure S29.[1]H NMR spectrum of Ti2a (400 MHz, C_6D_6)

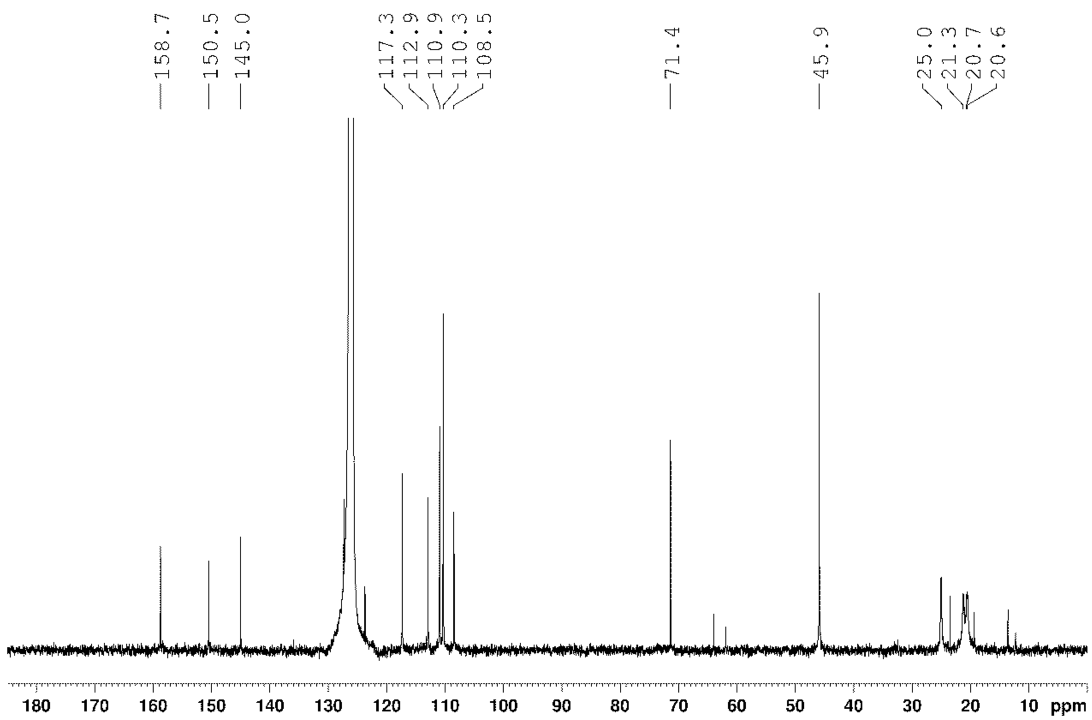

Figure S30.[13]C{[1]H} NMR spectrum of Ti2a (75 MHz, $CDCl_3$)

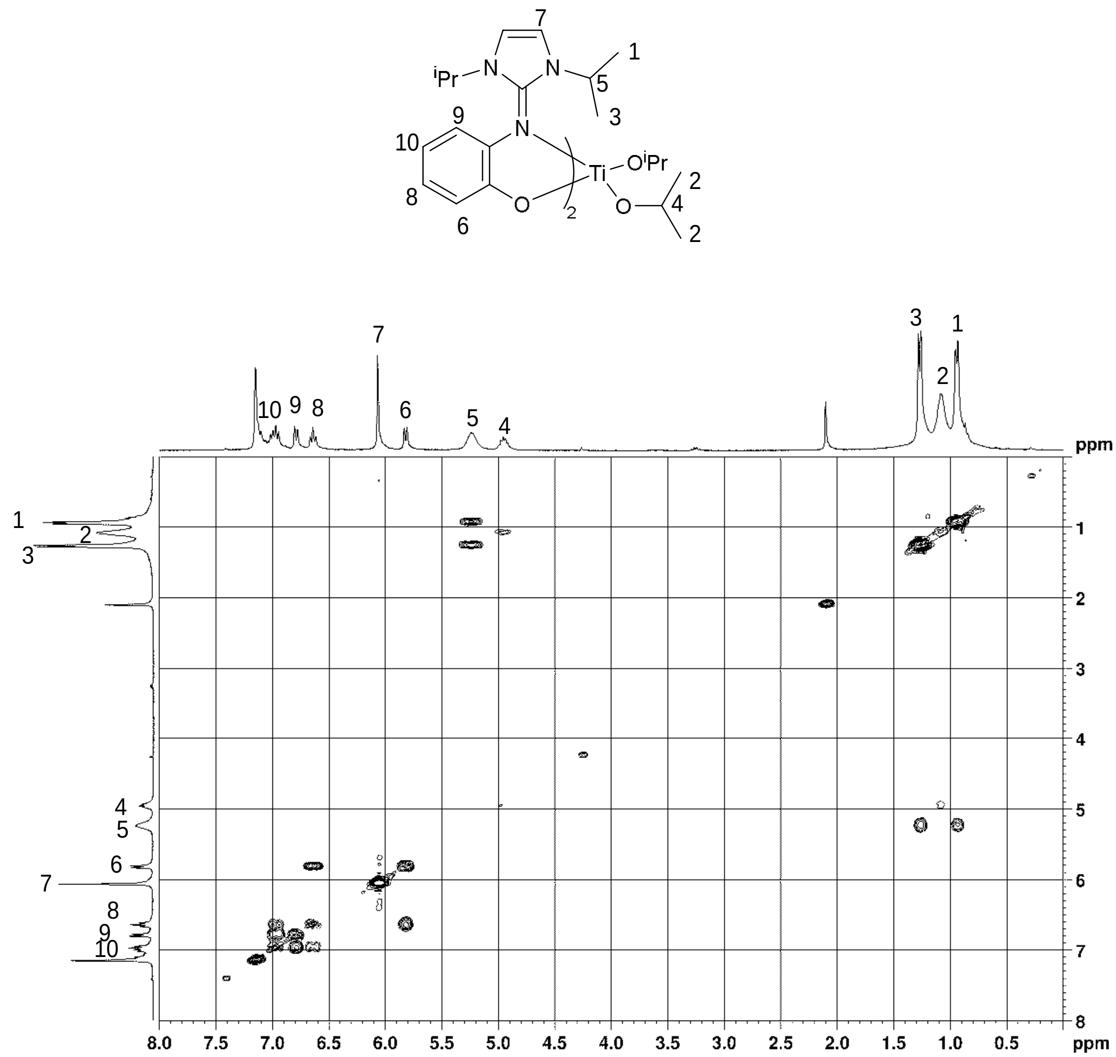

Figure S31. ^{1}H-^{1}H COSY spectrum of Ti2a (400 MHz, C_6D_6)

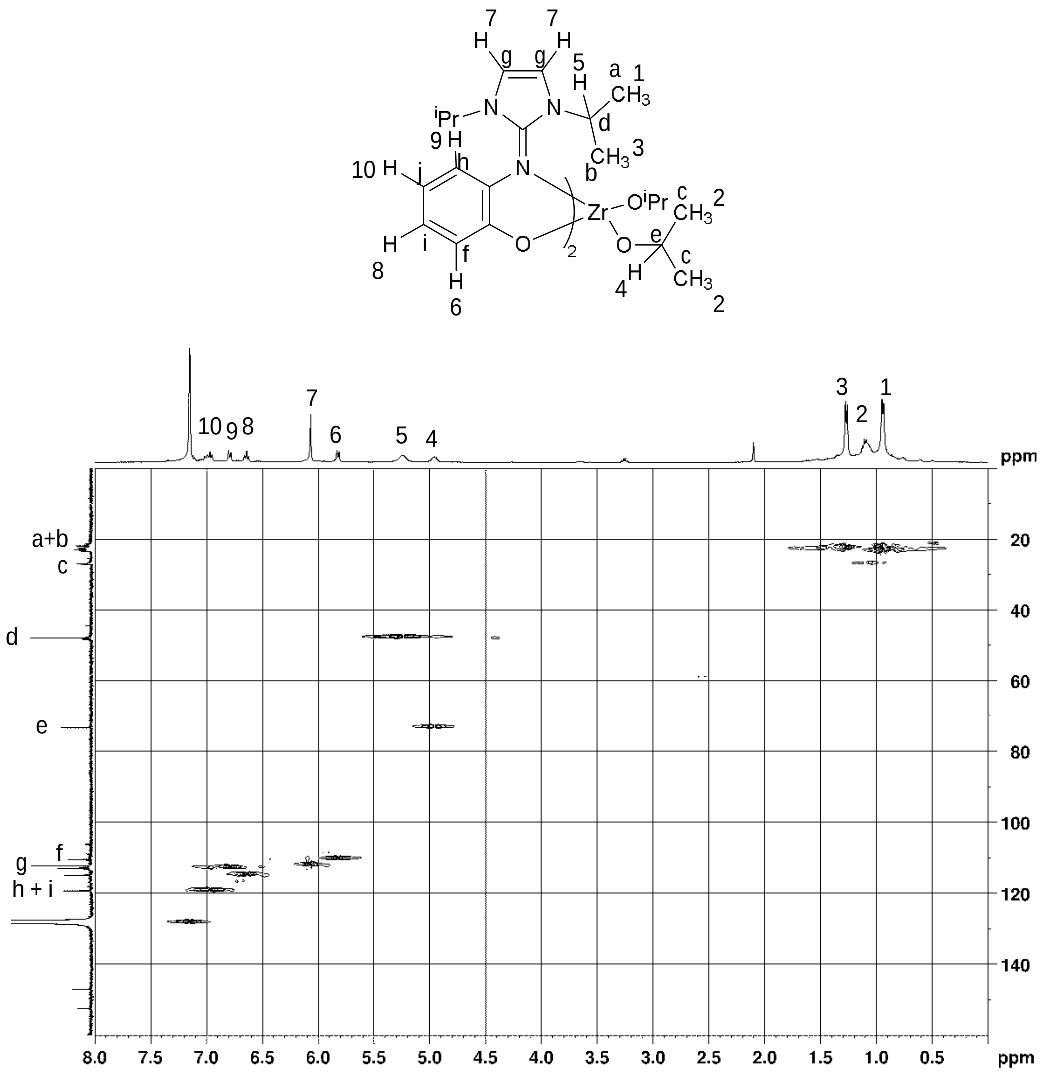

Figure S32. ^{1}H-^{13}C HSQC spectrum of Ti2a (400 MHz, C_6D_6)

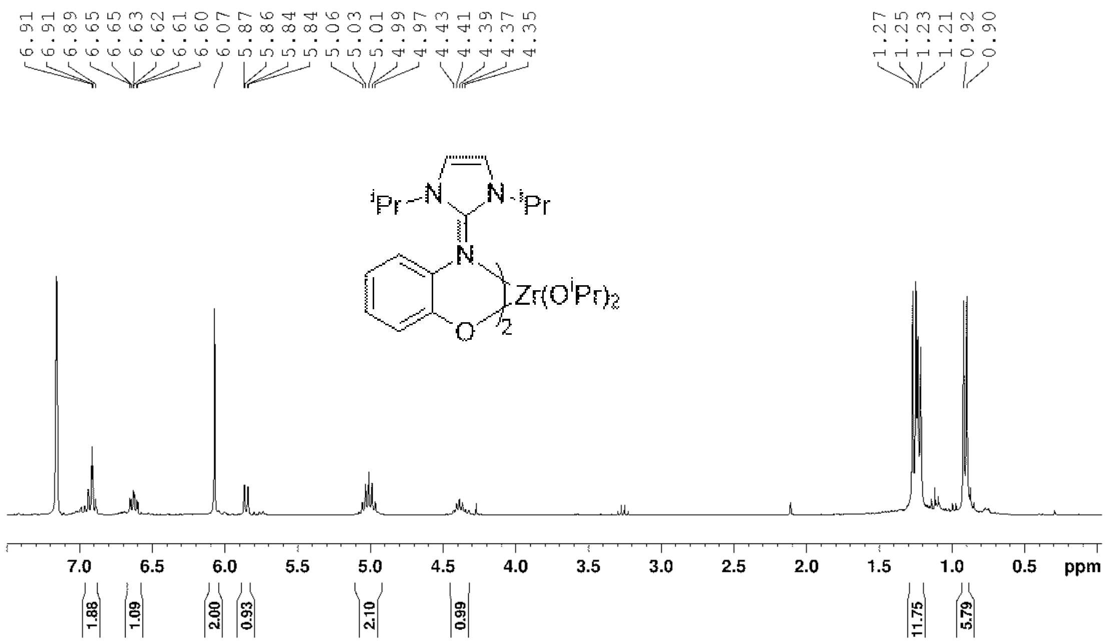

Figure S33.[1]H NMR spectrum of Zr2a (300 MHz, C_6D_6)

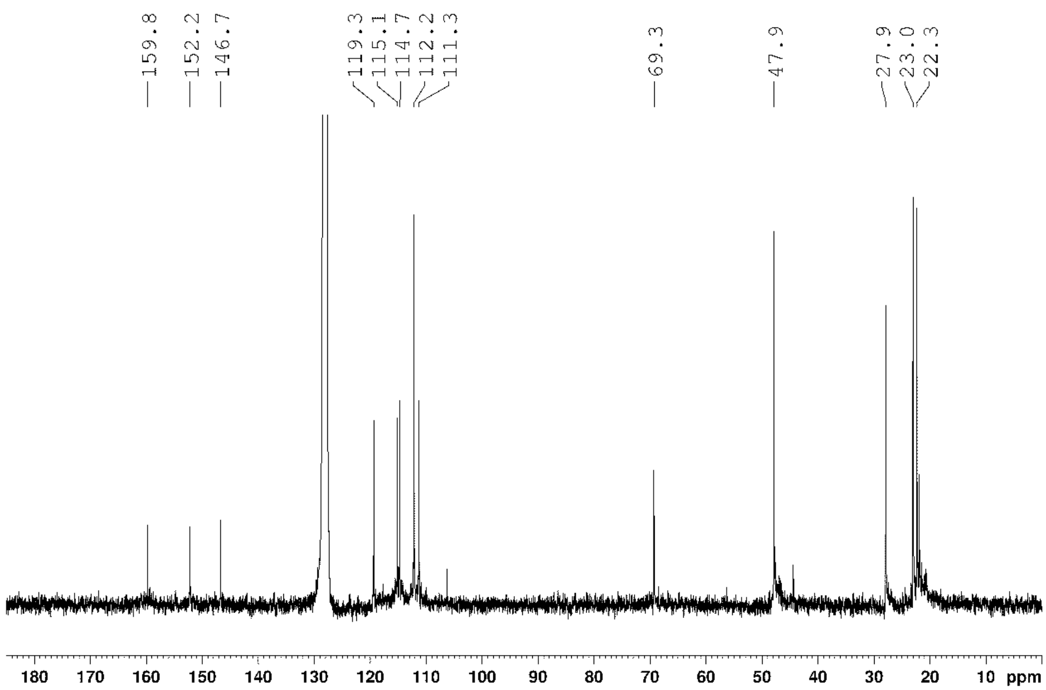

Figure S34.[13]C{[1]H} NMR spectrum of Zr2a (75 MHz, C_6D_6)

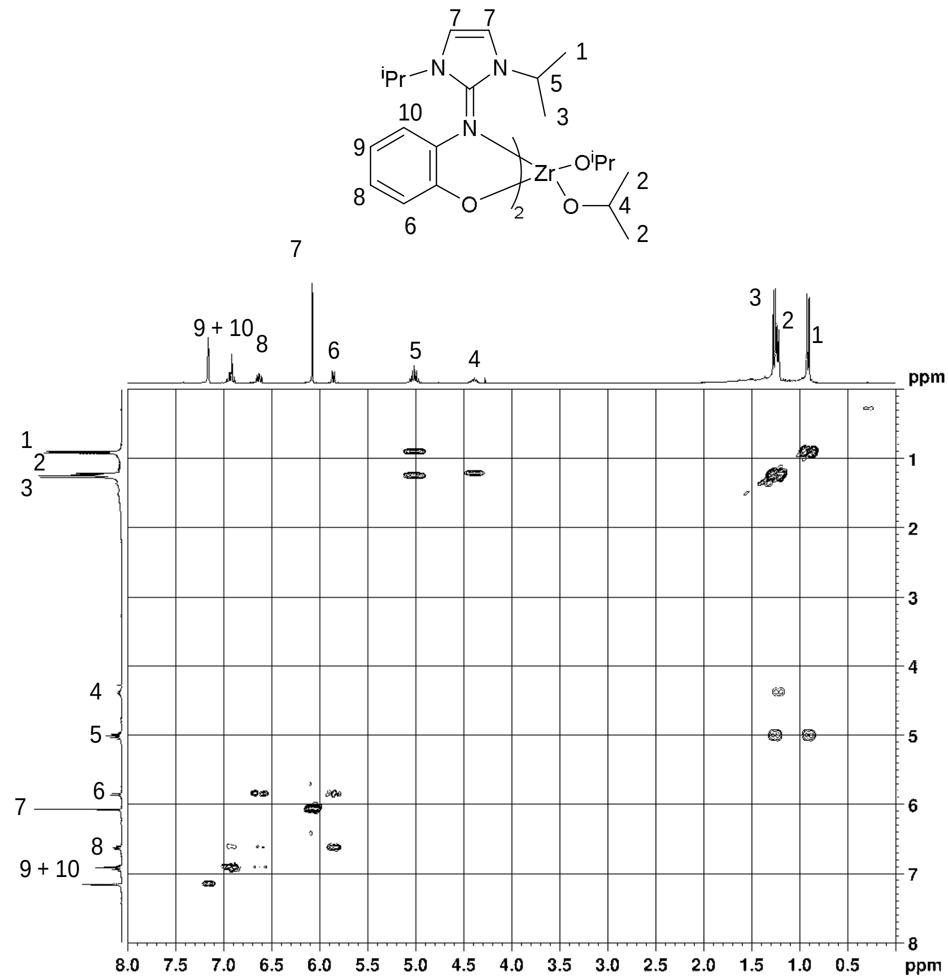

Figure S35. ^1H-^1H COSY spectrum of Zr2a (400 MHz, C_6D_6)

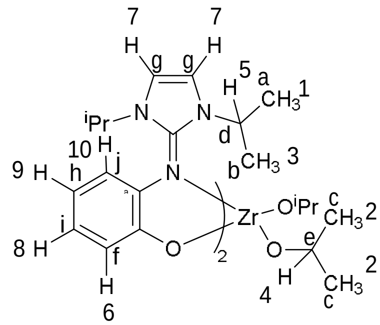

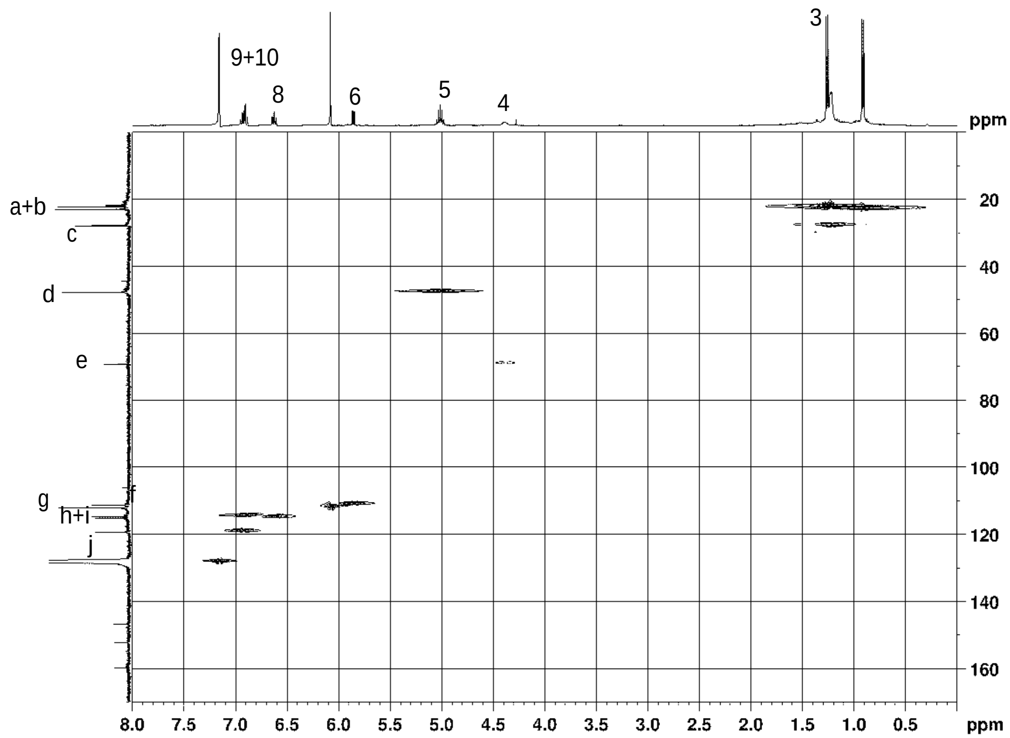

Figure S36. ^{1}H-^{13}C HSQC spectrum of Zr2a (400 MHz, C_6D_6)

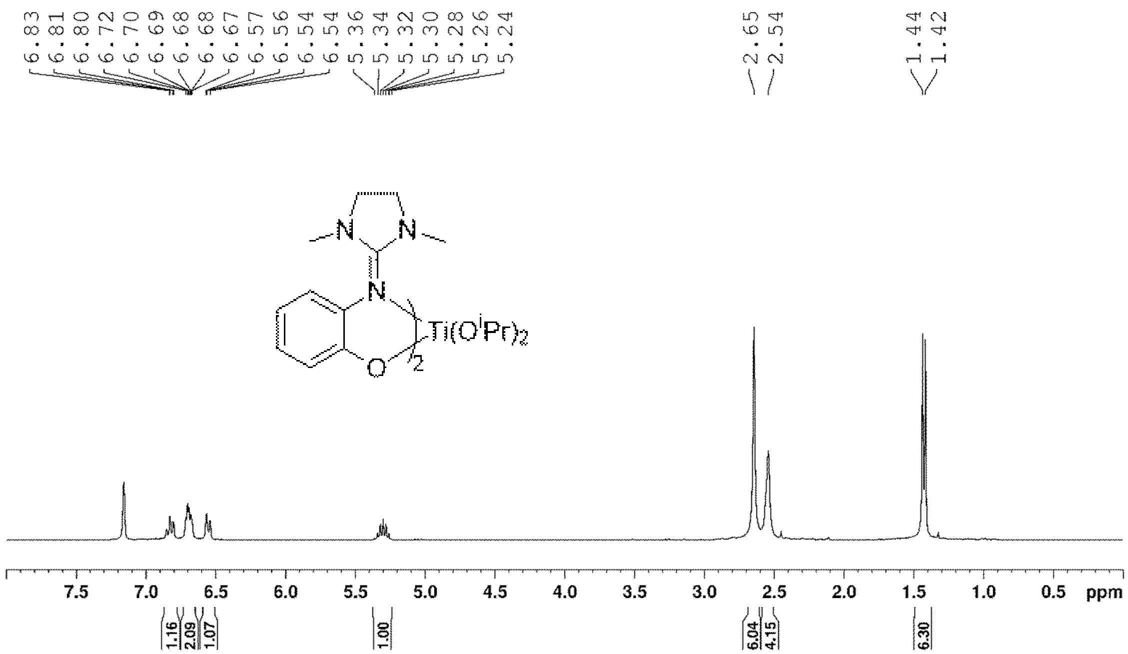

Figure S37.^{1}H NMR spectrum of Ti3a (300 MHz, C_6D_6)

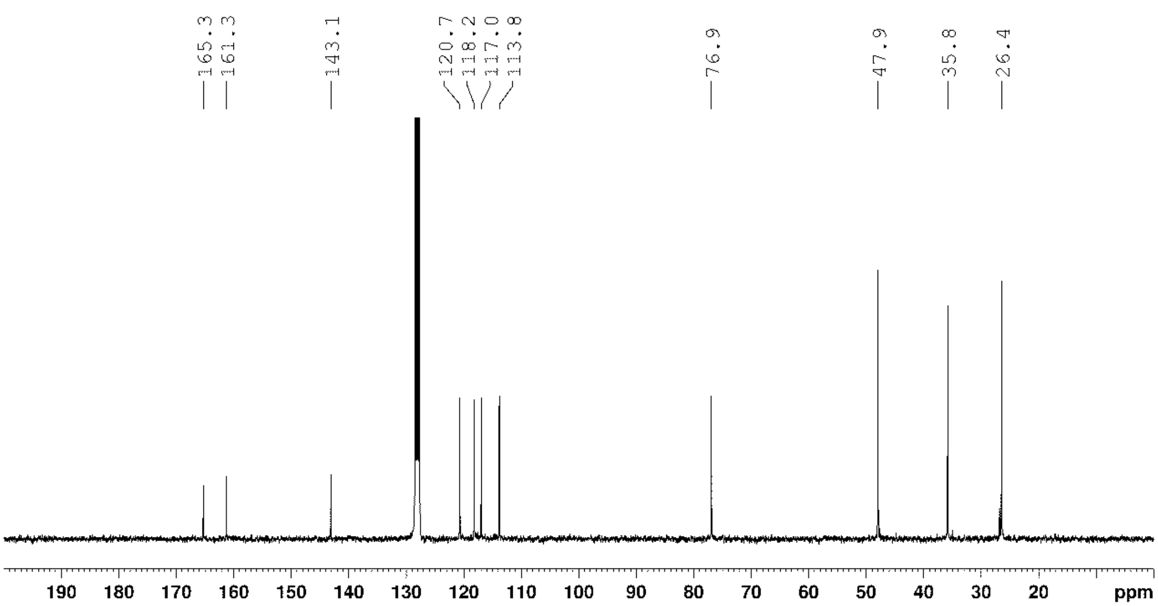

Figure S38.^{13}C{^{1}H} NMR spectrum of Ti3a (75 MHz, C_6D_6)

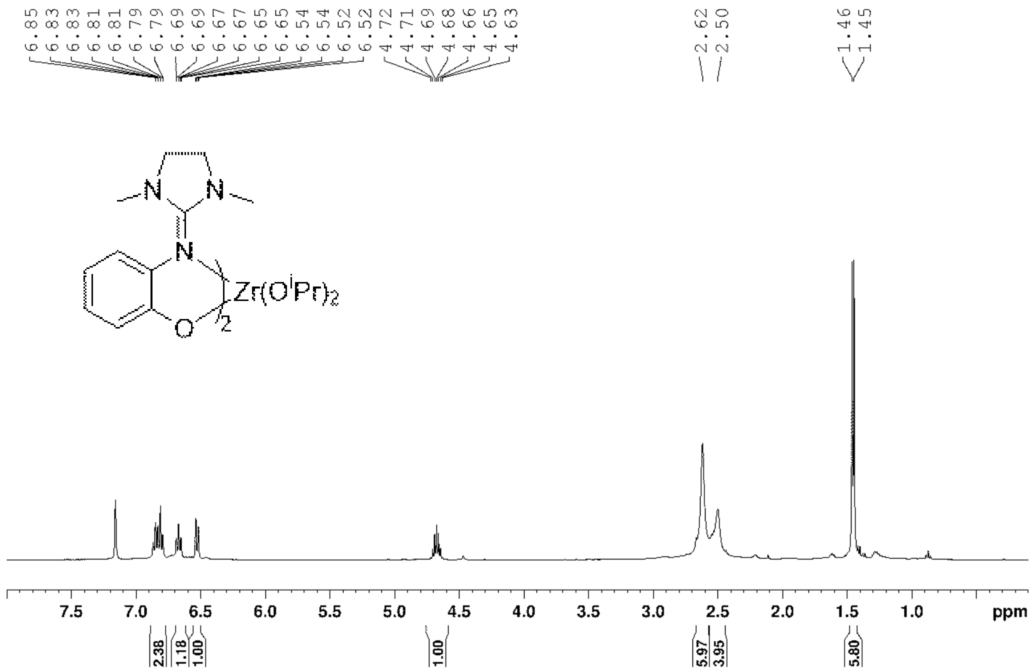

Figure S39.[1]H NMR spectrum of Zr3a (400 MHz, C_6D_6)

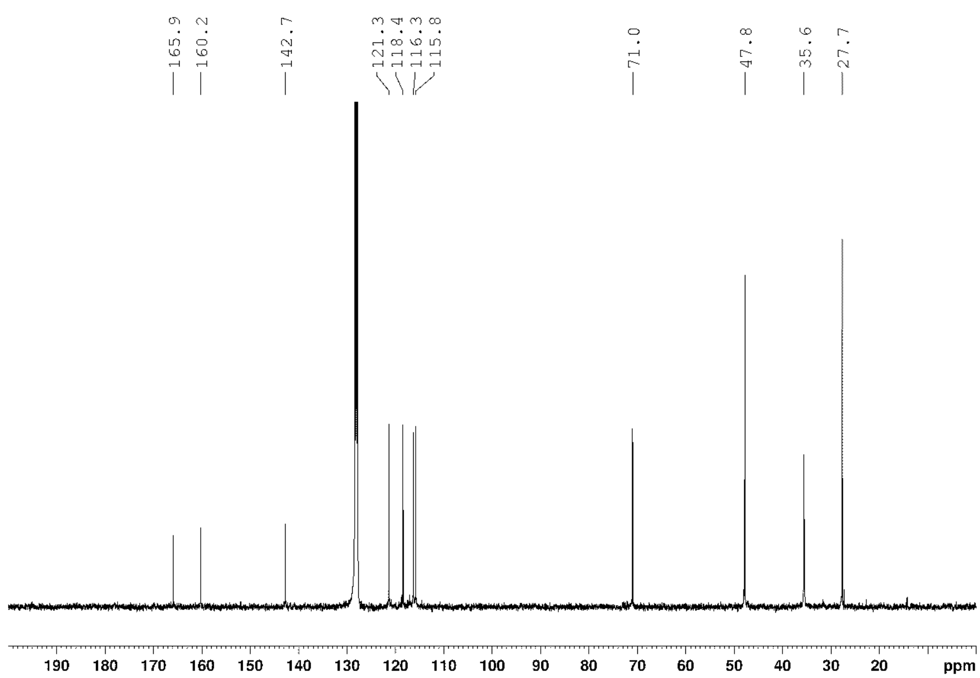

Figure S40.$^{13}C\{^1H\}$ NMR spectrum of Zr3a (100 MHz, C_6D_6)

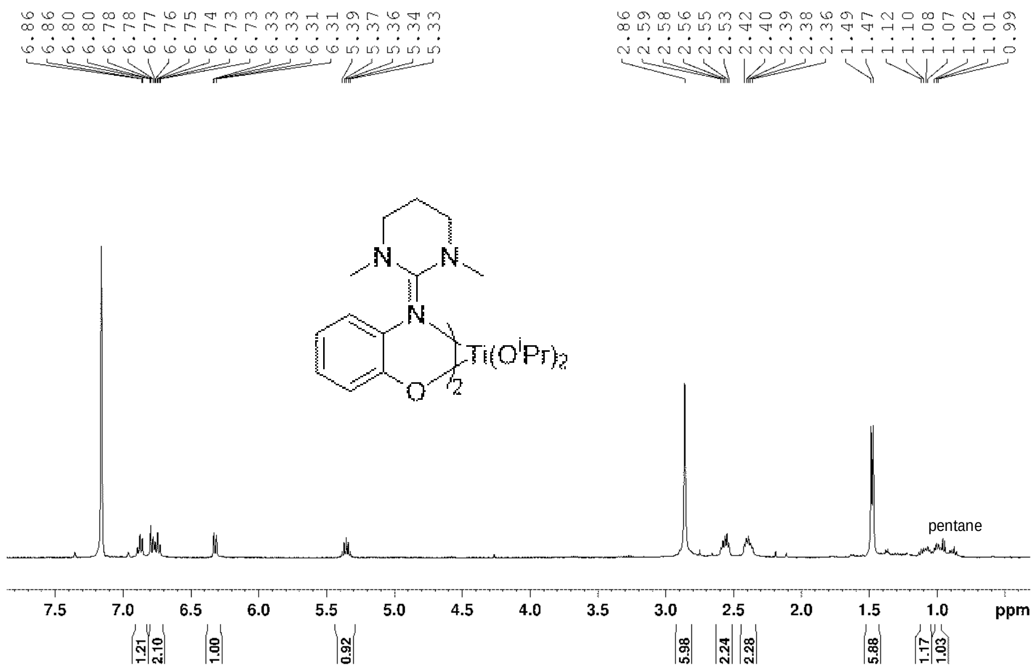

Figure S41.[1]H NMR spectrum of Ti4a (300 MHz, C_6D_6)

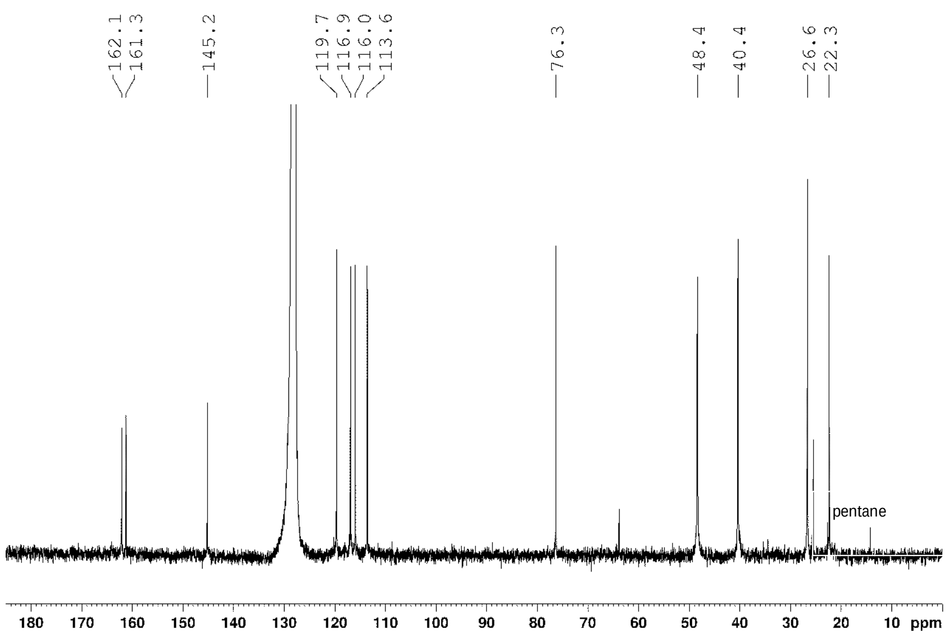

Figure S42.$^{13}C\{^1H\}$ NMR spectrum of Ti4a (75 MHz, C_6D_6)

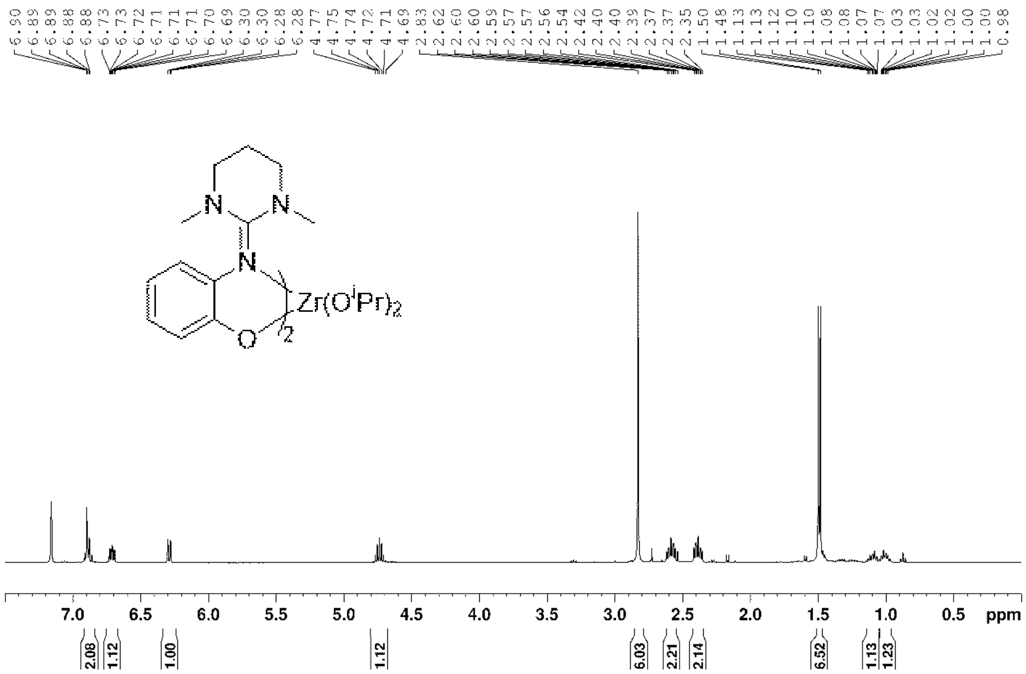

Figure S43.^{1}H NMR spectrum of Zr4a (400 MHz, C_6D_6)

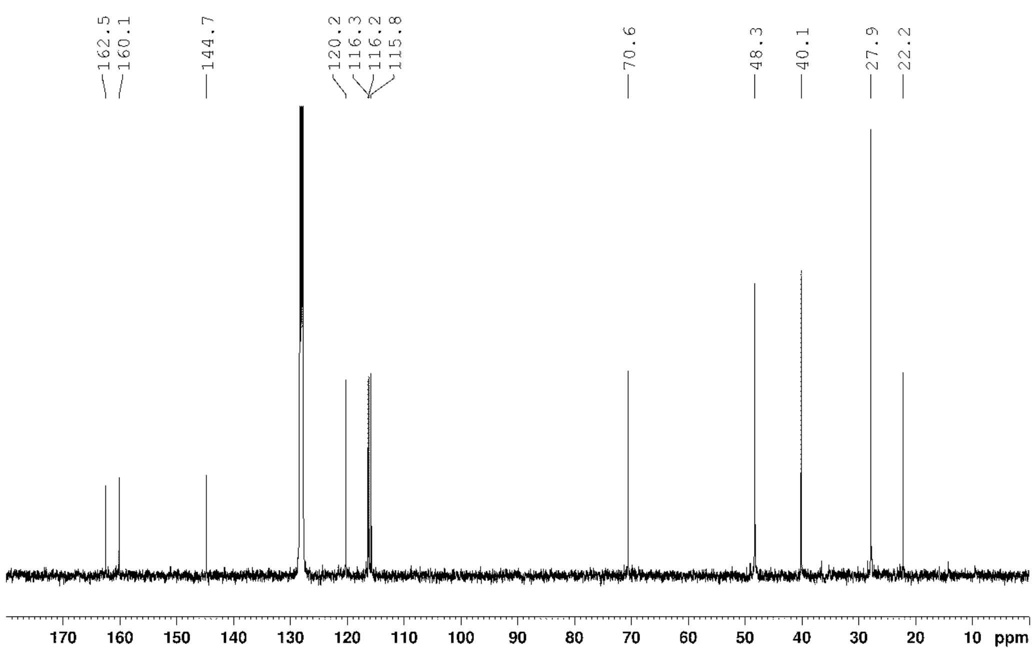

Figure S44.$^{13}C\{^1H\}$ NMR spectrum of Zr4a (100 MHz, C_6D_6)

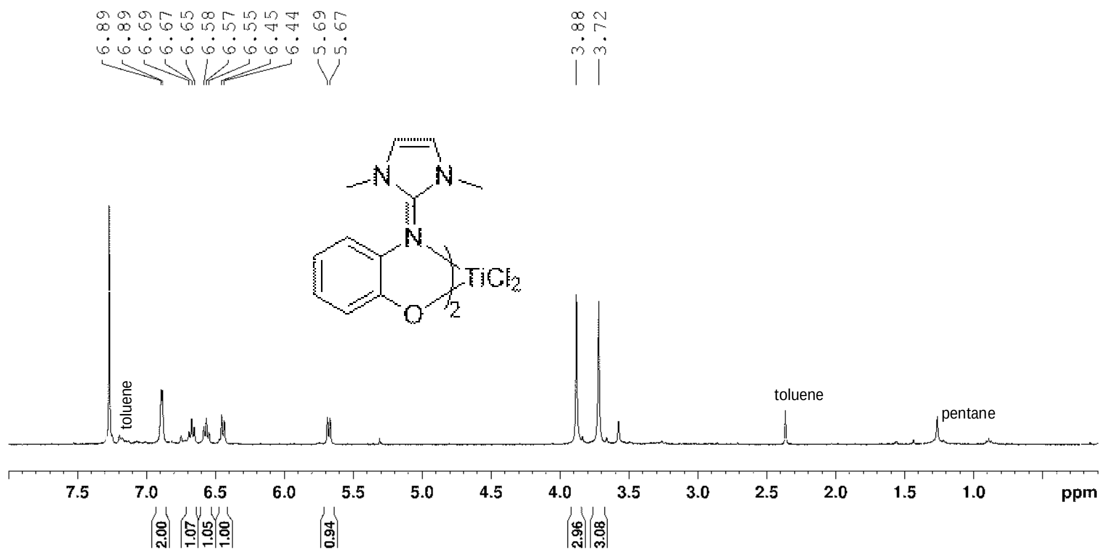

Figure S45.[1]H NMR spectrum of Ti1b (400 MHz, C_6D_6)

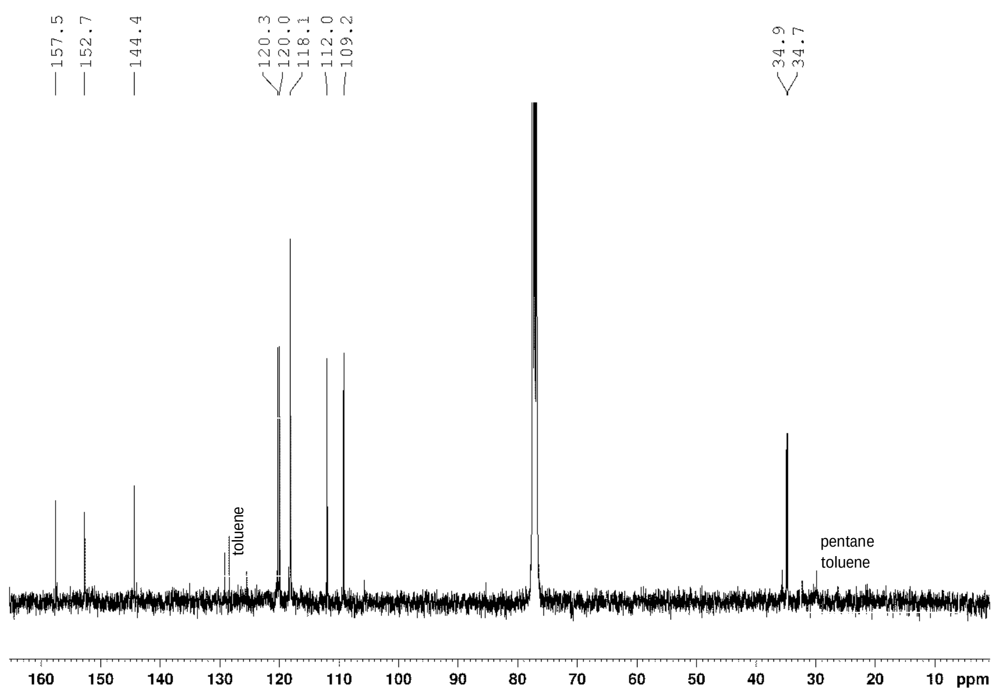

Figure S46.[13]C{[1]H} NMR spectrum of Ti1b (100 MHz, C_6D_6)

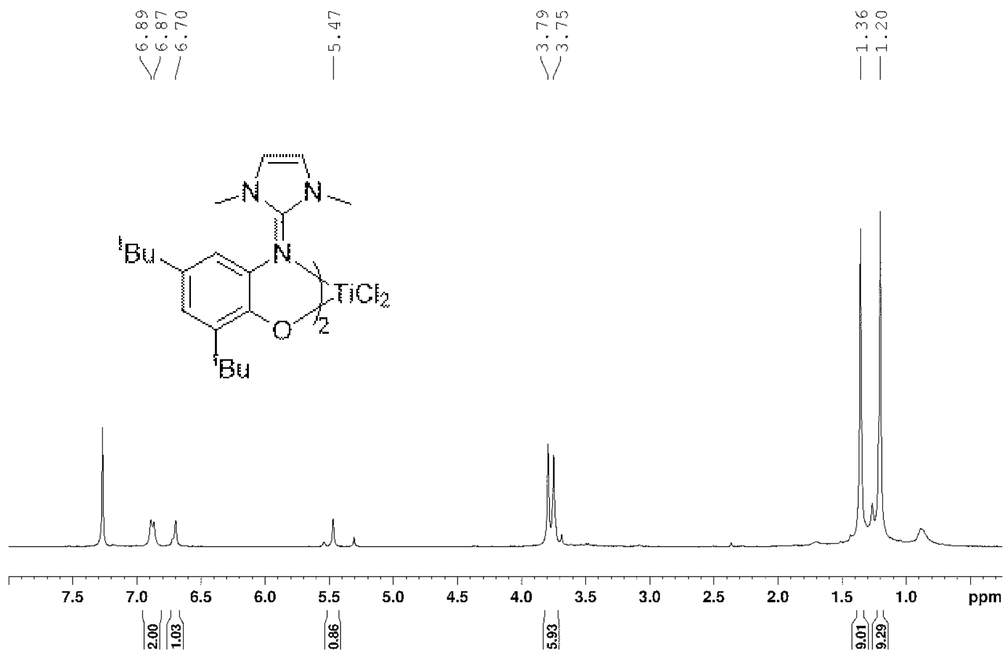

Figure S47.^{1}H NMR spectrum of Ti1′b (400 MHz, $CDCl_3$)

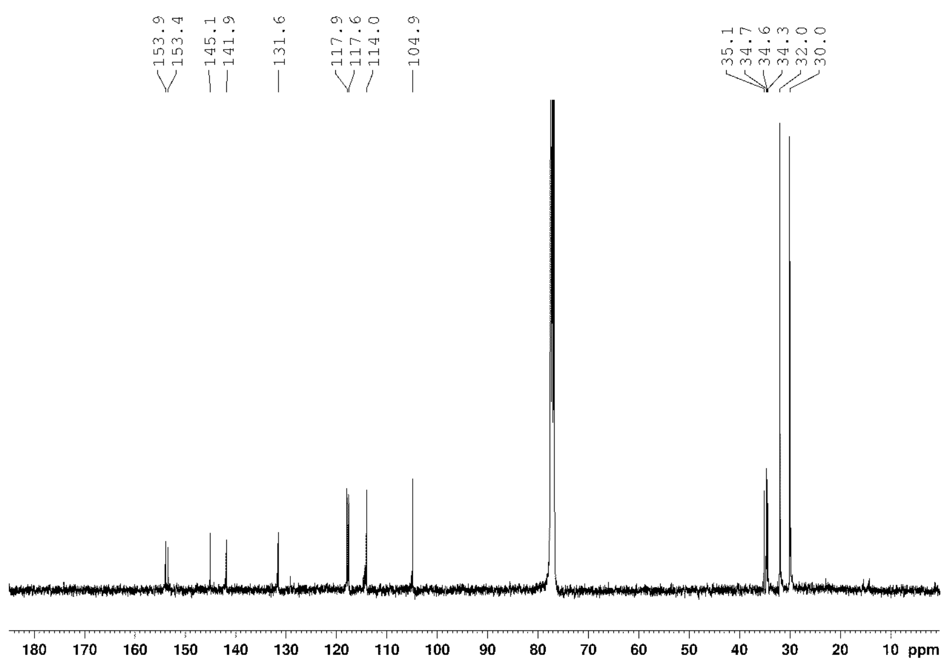

Figure S48.$^{13}C\{^{1}H\}$ NMR spectrum of Ti1′b (100 MHz, $CDCl_3$)

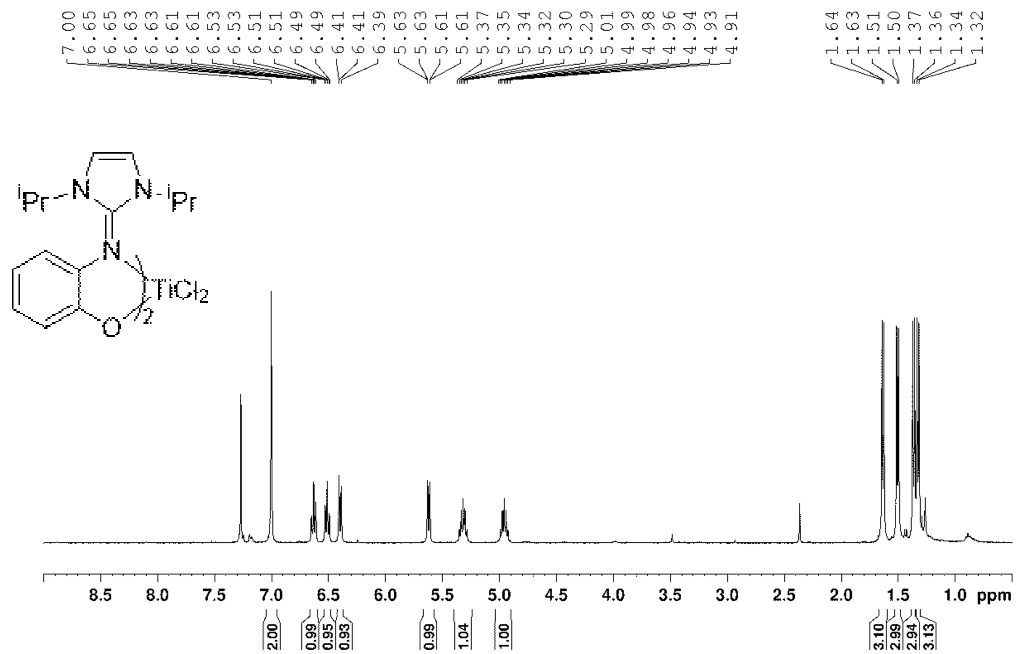

Figure S49.[1]H NMR spectrum of Ti2b (400 MHz, $CDCl_3$)

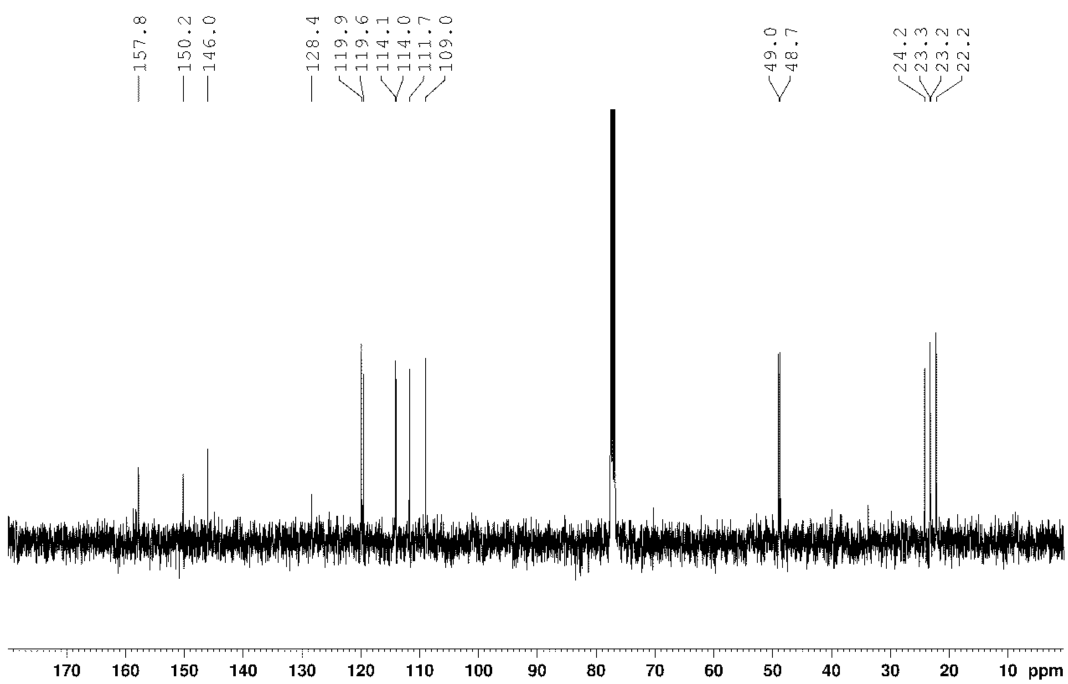

Figure S50.$^{13}C\{^1H\}$ NMR spectrum of Ti2b (100 MHz, $CDCl_3$)

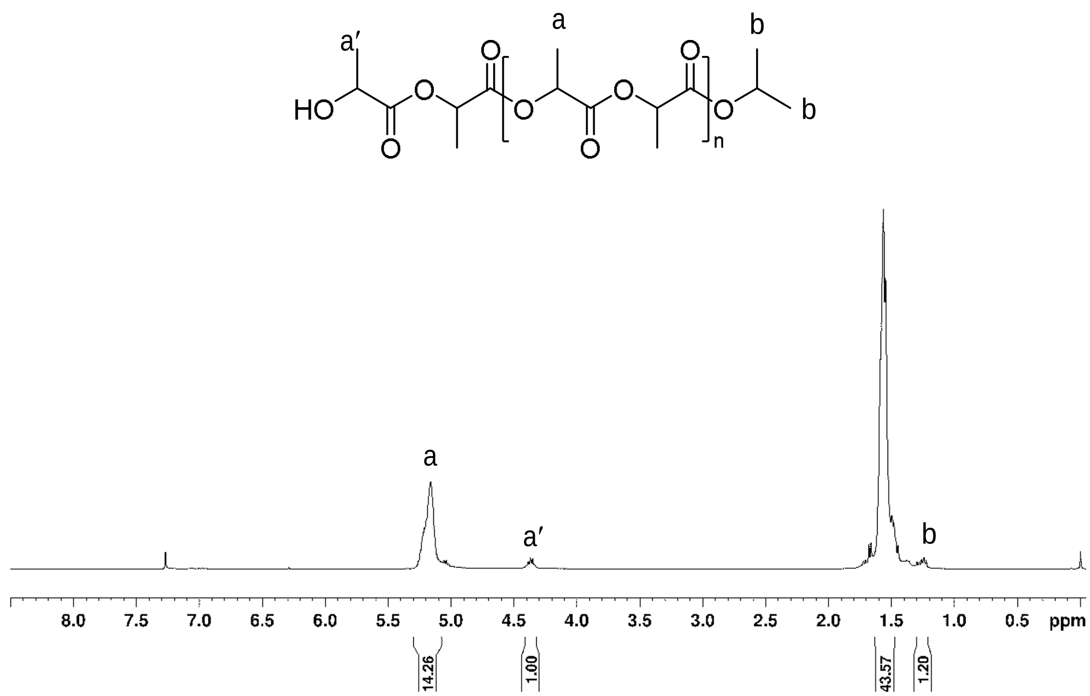

Figure S51.[1]H NMR spectrum of the polymer produced with Zr2a (400 MHz, $CDCl_3$)

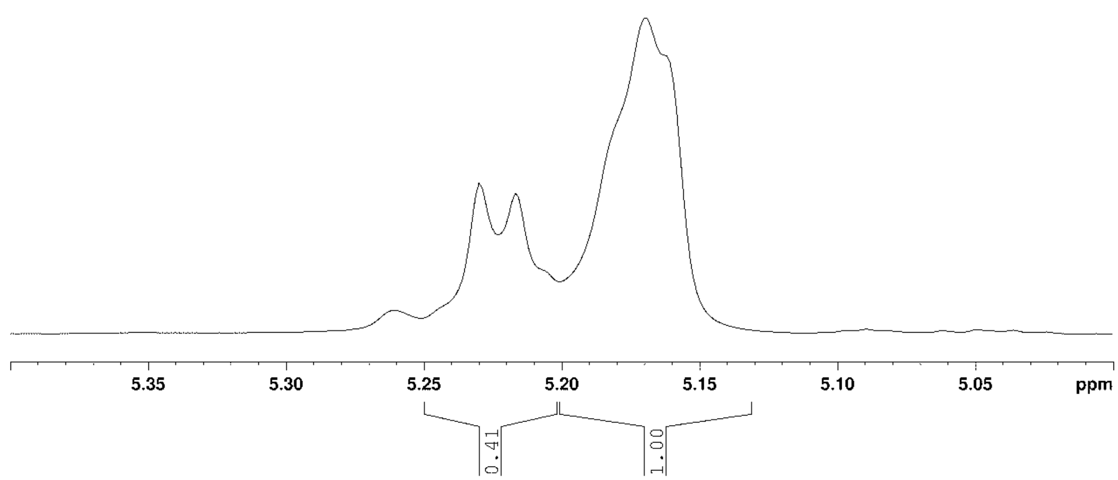

Figure S52.Homonuclear-decoupled [1]H NMR spectrum of the polymer produced with Zr2a (400 MHz, $CDCl_3$)

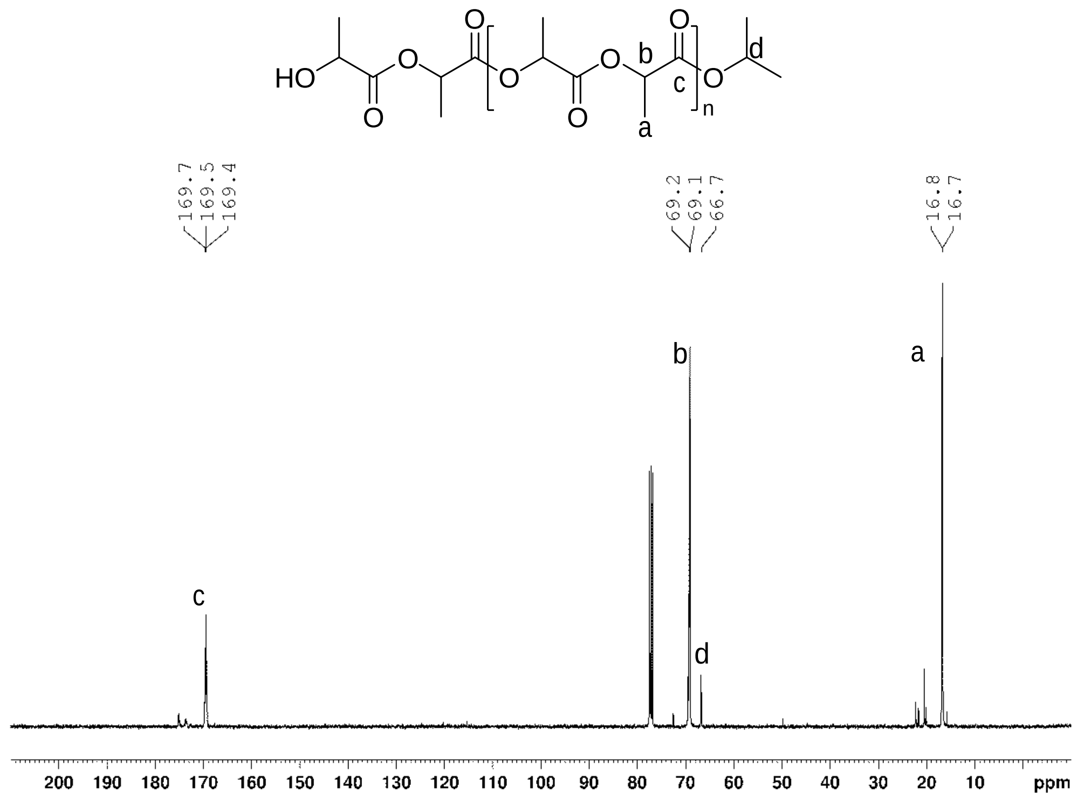

Figure S53. $^{13}C\{^{1}H\}$ spectrum of the polymer produced with Zr2a (100 MHz, $CDCl_3$)

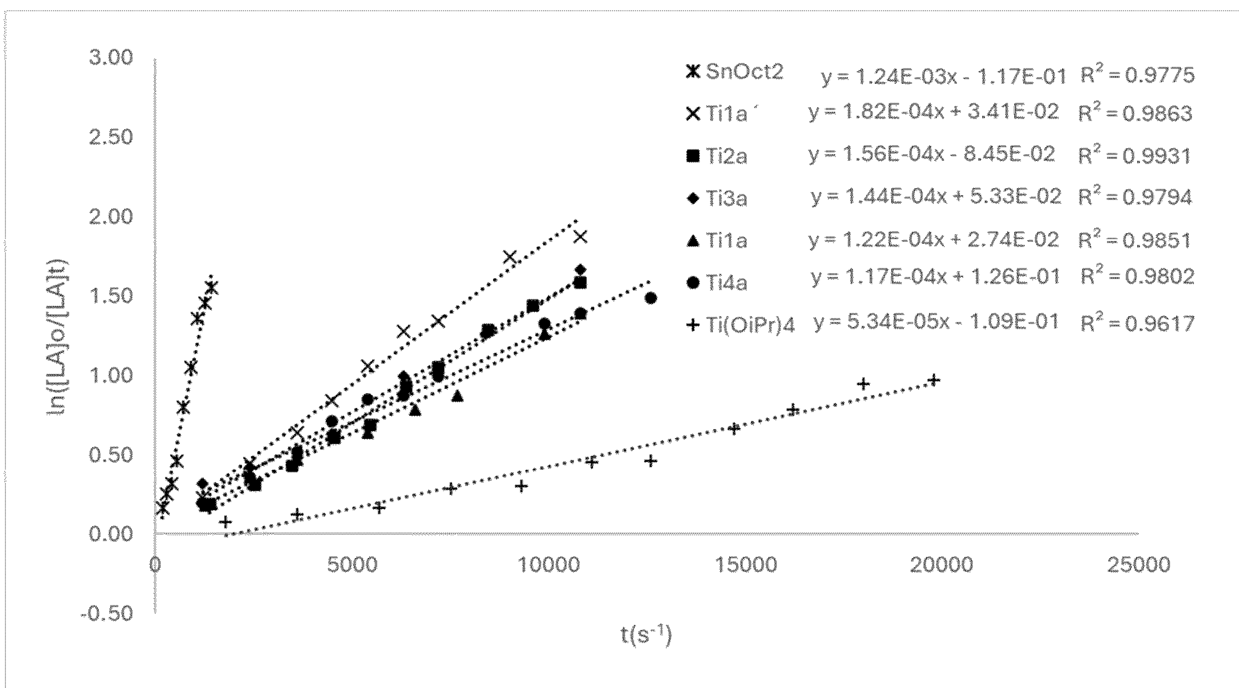

Figure S54. Kinetic plot for the polymerization of rac-lactide by $Sn(Oct)_2$, $Ti(OiPr)_4$, Ti1a, Ti1′a, Ti2a, Ti3a, and Ti4a.

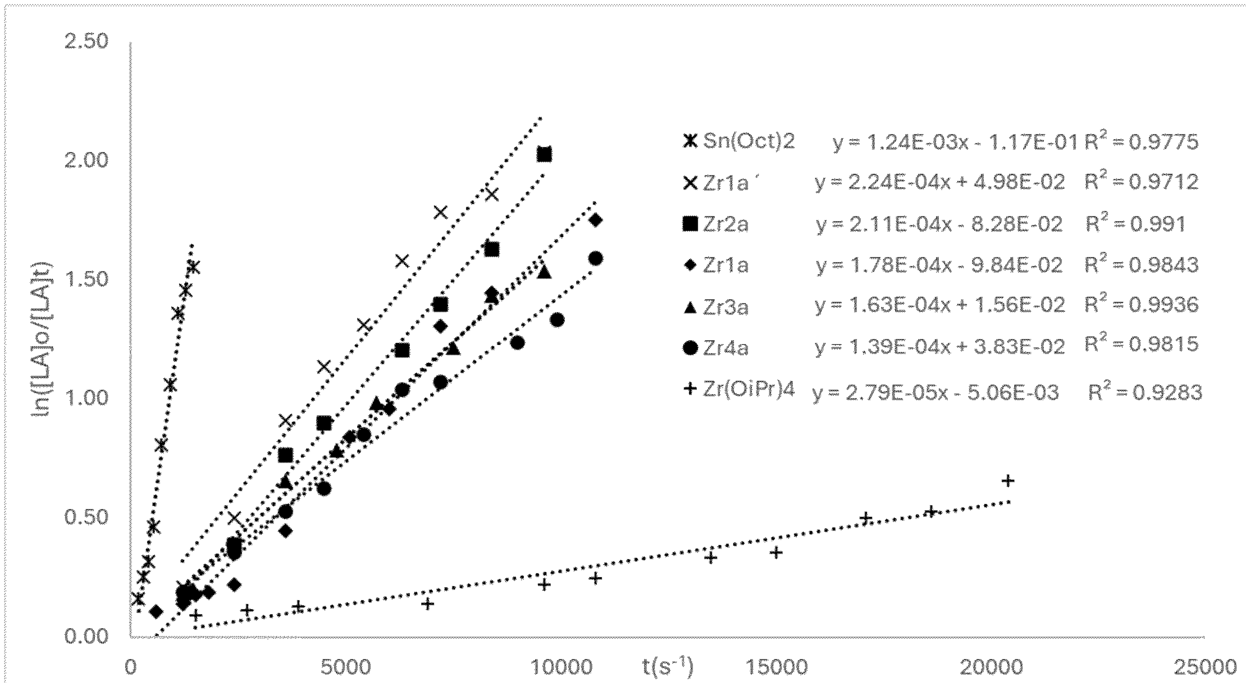

Figure S55. Kinetic plot for the polymerization of *rac*-lactide by $Sn(Oct)_2$, $Zr(OiPr)_4 \cdot {}^iPrOH$, Zr1a, Zr1′a, Zr2a, Zr3a, and Zr4a.

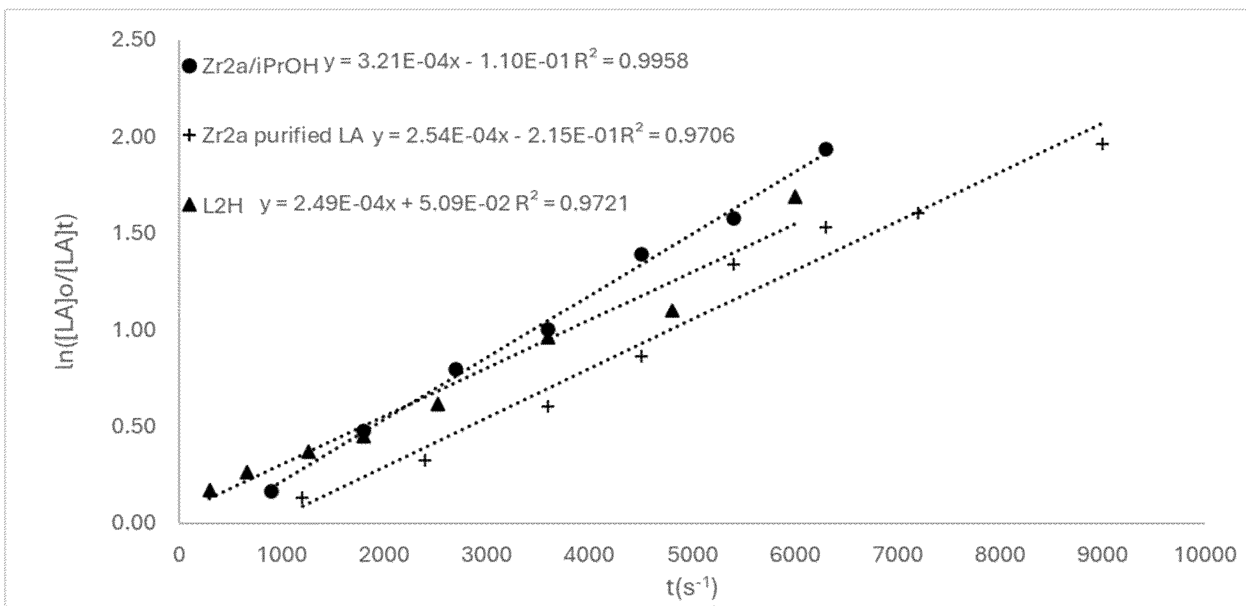

Figure S56. Kinetic plot for the polymerization of *rac*-lactide by L2H, Zr2a with purified monomer and Zr2a + ^iPrOH.

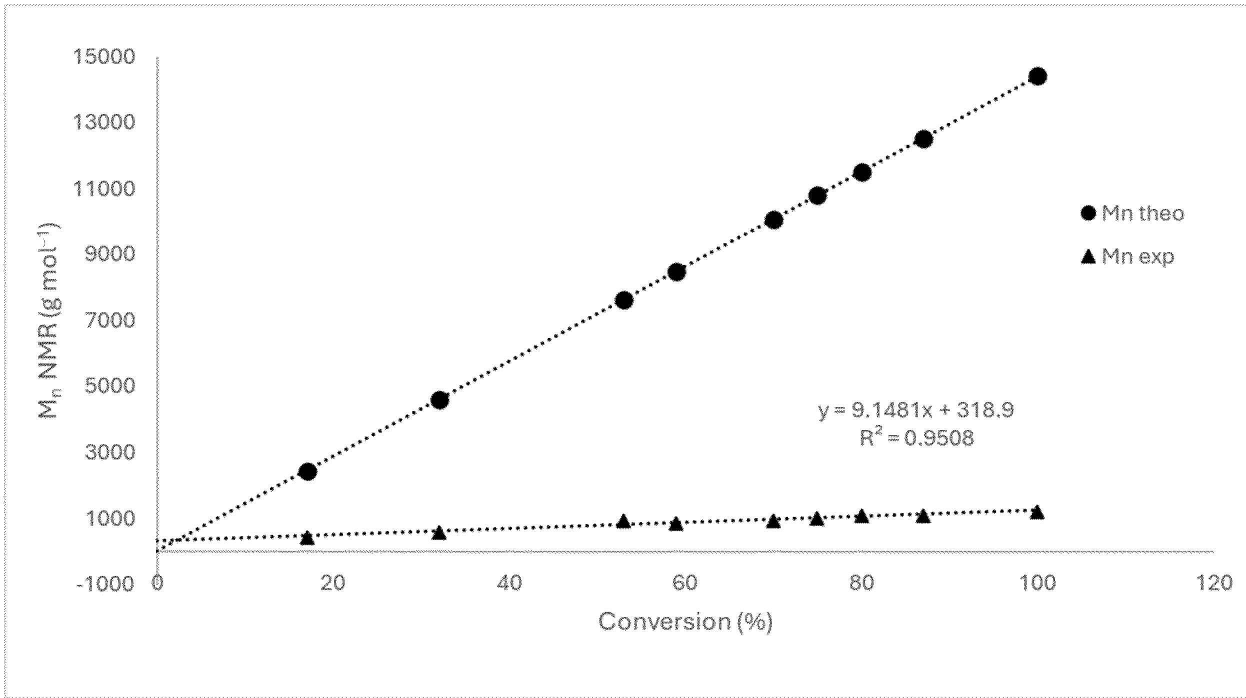

Figure S57. Number-average molecular weight of PLA produced by Zr2a as a function of conversion. The triangles (▲) represent the M_n measured by NMR end-group analysis. The circles (●) represent the theoretical M_n based on the initial LA:Zr ratio, assuming a living system.

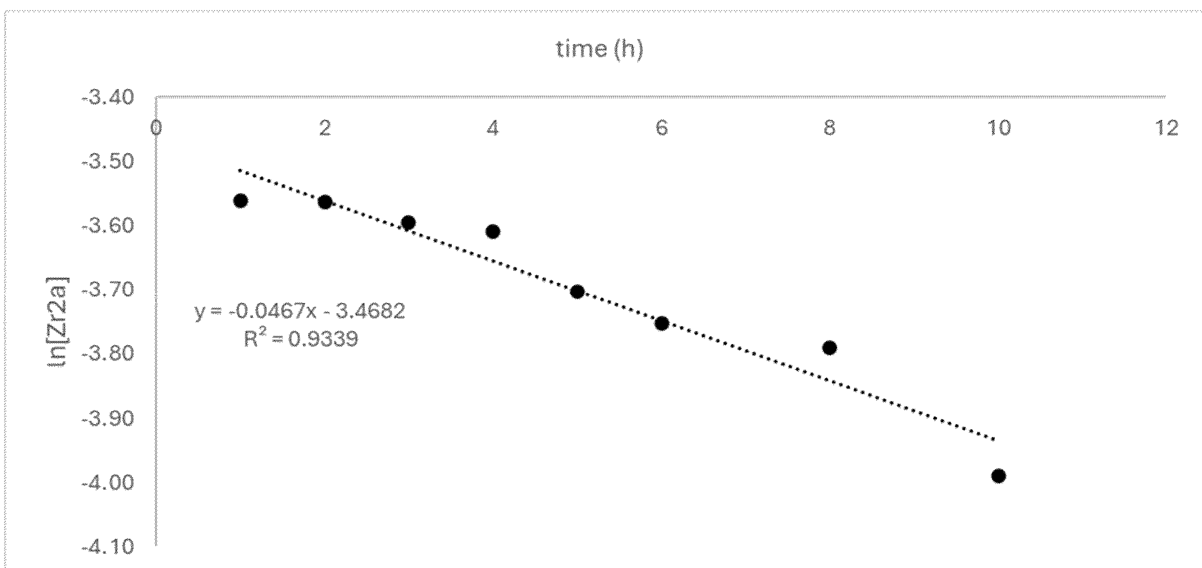

Figure S58. Decay Zr2a as a function of time when dissolved in toluene and heated to 120 °C.

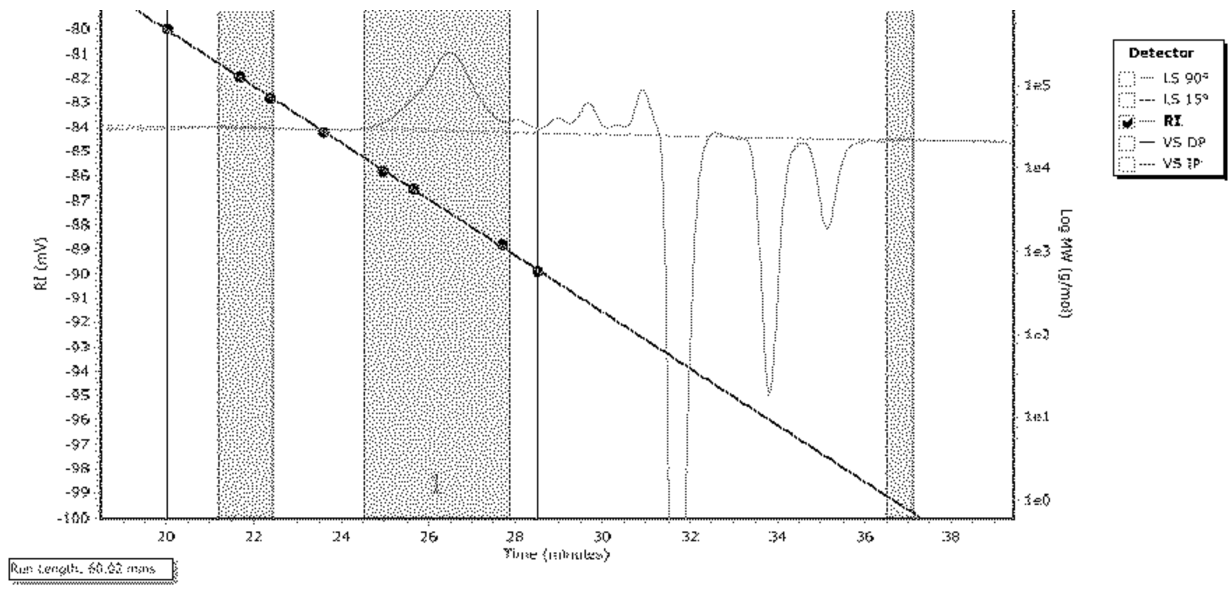

Figure S59. Representative GPC chromatogram plot of a polymer sample, herein obtained using complex Zr1a (entry 6).

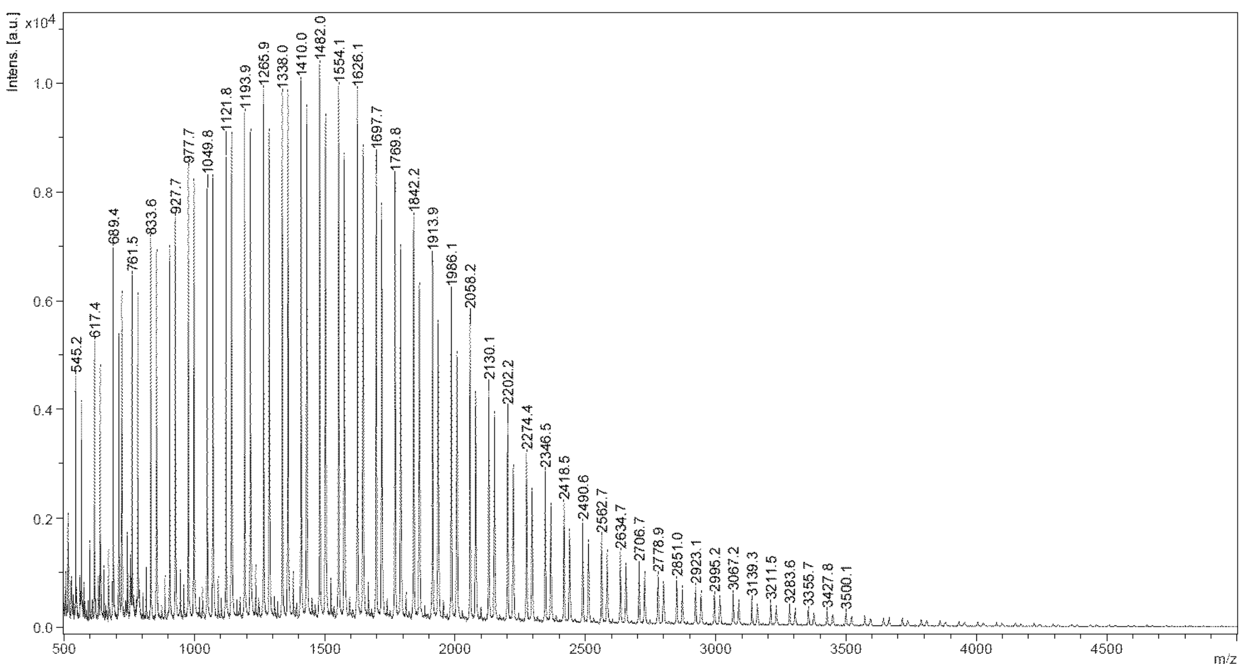

Figure S60. MALDI-TOF mass spectrum of the polymer obtained using complex Ti2a.

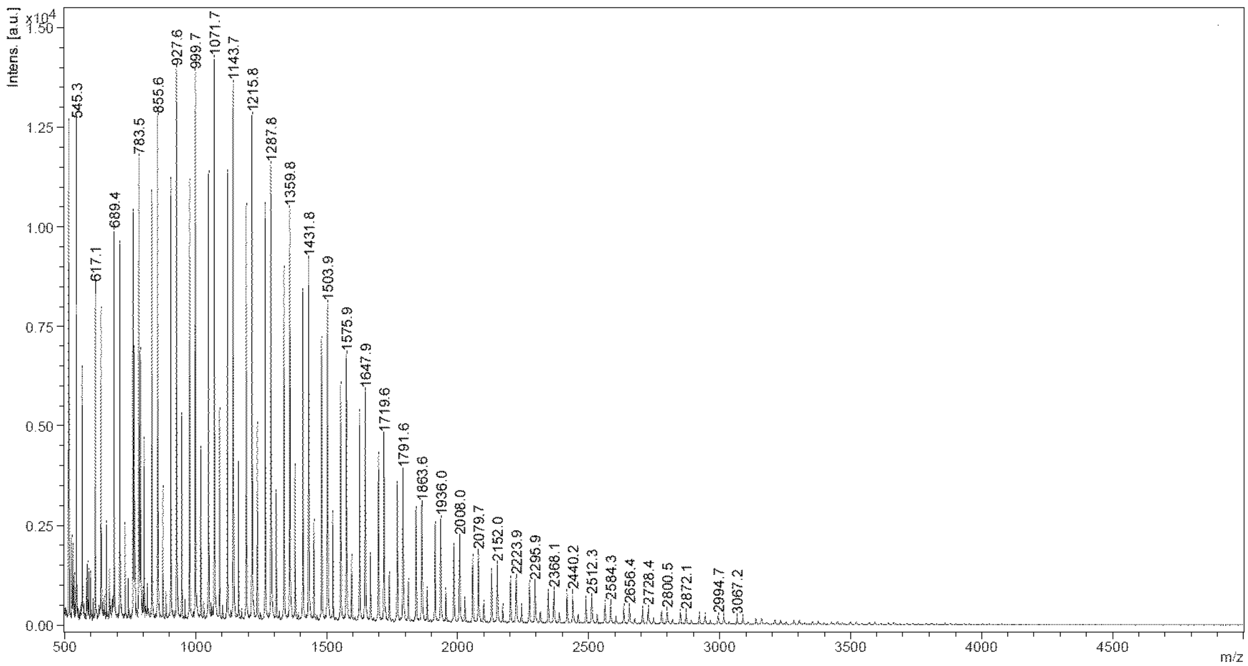

Figure S61. MALDI-TOF mass spectrum of the polymer obtained using complex Zr2a.

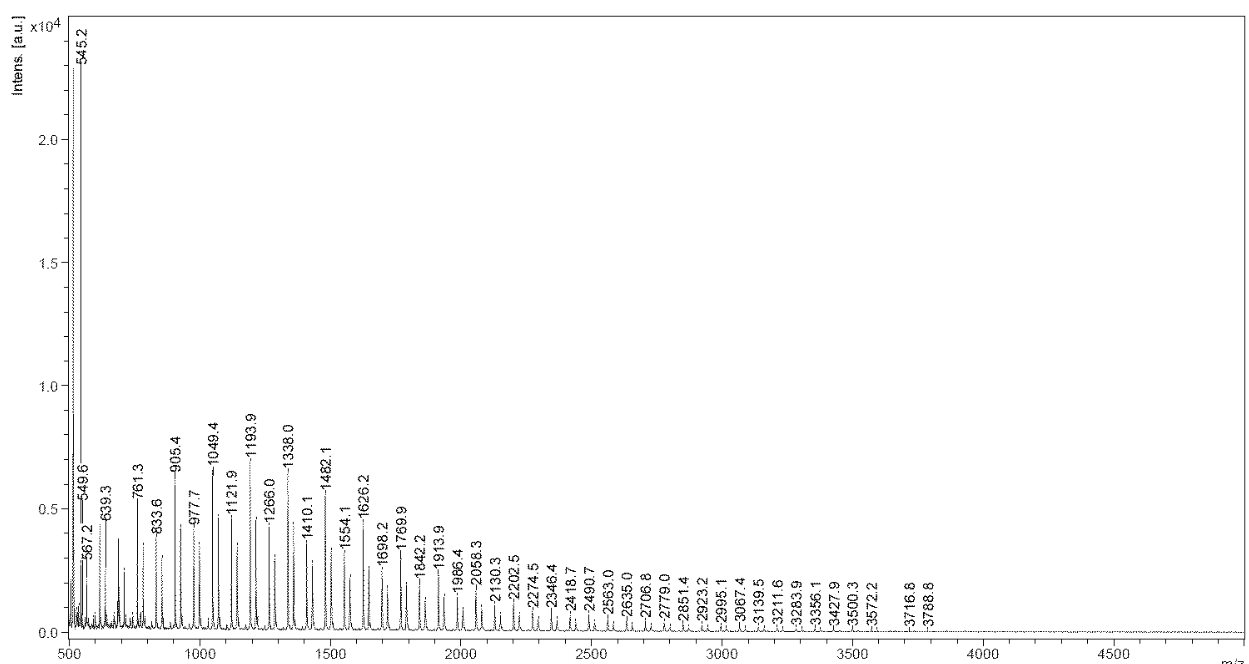

Figure S62. MALDI-TOF mass spectrum of the polymer obtained using complex L2H.

Table S1. Relative energies (kJ mol^{-1}) of the five diastereoisomers for the bis(alkoxide) complexes Ti3a , Zr3a, and Ti4a

Complex	*cis*-O^iPr			*trans*- O^iPr	
	cis-N,N-*trans*-O,O	*cis*-N,N-*cis*-O,O	*trans*-N,N-*cis*-O,O	*cis*-N,N-*cis*-O,O	*trans*-N,N-*trans*-O,O
Ti3a	0.0	5	15	46	50
Zr3a	0.0	1	15	44	35
Ti4a	0.0	28	27	70	62

Table S2. Rate constant of the polymerization of *rac*-lactide

entry[a]	Catalyst	k_{app} (10^{-5} s^{-1})	M_n[b] (Da)	M_w[b] (Da)	*Đ*[c]
1	**Ti2a**	1.42	2600	3600	1.4
2	**Zr2a**	2.03	2100	2900	1.4
3	**L2H**[d]	0.92	2800	3900	1.4

[a]All polymerization were carried out at 130 °C to full conversion and a lactide-to-catalyst stoichiometric ratio of 1000:1. [b]Determined by GPC in THF [c]$Đ = M_w \div M_n$ as determined by GPC [d]Lactide:catalyst stoichiometric ratio of 500:1.

Table S3. Crystal data for Ti3a

Empirical formula	$C_{28}H_{42}N_6O_4Ti$
Formula weight	574.57
Temperature/ K	173.0
Crystal system	monoclinic
Space group	P21/n
a/Å	23.2014(7)
b/Å	10.7004(3)
c/Å	24.3975(7)
α/°	90
β/°	95.7949(12)
γ/°	90
Volume/Å3	6026.1(3)
Z	8
ρcalcg/cm3	1.267
μ/mm-1	0.326
F(000)	2448.0
Crystal size/mm3	0.1 × 0.1 × 0.1
Radiation	MoKα (λ = 0.71073)
2Θ range for data collection/°	5.076 to 60.066
Index ranges	-29 ≤ h ≤ 32, -15 ≤ k ≤ 15, -34 ≤ l ≤ 34
Reflections collected	157194
Independent reflections	17589 [Rint = 0.0771, Rsigma = 0.0307]
Data/restraints/parameters	17589/0/779
Goodness-of-fit on F2	1.131
Final R indexes [I>=2σ (I)]	R1 = 0.0532, wR2 = 0.1254
Final R indexes [all data]	R1 = 0.0643, wR2 = 0.1316
Largest diff. peak/hole /	e Å-3 0.43/-0.60

Table S4. Crystal data for Zr3a

Empirical formula	$C_{28}H_{42}N_6O_4Zr$
Formula weight	617.89
Temperature/K	173.00
Crystal system	monoclinic
Space group	$P2_1/n$
a/Å	9.6548(4)
b/Å	15.7838(6)
c/Å	19.7193(7)
α/°	90
β/°	90.246(2)
γ/°	90
Volume/Å^3	3005.0(2)
Z	4
ρ_{calc}g/cm^3	1.366
μ/mm^{-1}	0.408
F(000)	1296.0
Crystal size/mm^3	0.4 × 0.4 × 0.1
Radiation	MoKα (λ = 0.71073)
2Θ range for data collection/°	4.218 to 55.134
Index ranges	$-12 \leq h \leq 12$, $-20 \leq k \leq 20$, $-25 \leq l \leq 25$
Reflections collected	94441
Independent reflections	6938 [R_{int} = 0.1255, R_{sigma} = 0.0549]
Data/restraints/parameters	6938/0/371
Goodness-of-fit on F^2	1.049
Final R indexes [I>=2σ (I)]	R_1 = 0.0579, wR_2 = 0.0989
Final R indexes [all data]	R_1 = 0.0975, wR_2 = 0.1138
Largest diff. peak/hole / e Å^{-3}	1.10/-0.79

Table S5. Crystal data for Ti4a

Empirical formula	$C_{30}H_{46}N_6O_4Ti$
Formula weight	602.63
Temperature/K	173.00
Crystal system	orthorhombic
Space group	$Pca2_1$
a/Å	14.5172(8)
b/Å	11.5840(6)
c/Å	19.1268(10)
α/°	90
β/°	90
γ/°	90
Volume/Å^3	3216.5(3)
Z	4
ρ_{calc}g/cm^3	1.244
μ/mm^{-1}	0.309
F(000)	1288.0
Crystal size/mm^3	0.2 × 0.2 × 0.1
Radiation	MoKα (λ = 0.71073)
2Θ range for data collection/°	4.498 to 55.106
Index ranges	$-18 \leq h \leq 18, -14 \leq k \leq 15, -24 \leq l \leq 24$
Reflections collected	39189
Independent reflections	7358 [R_{int} = 0.0835, R_{sigma} = 0.0610]
Data/restraints/parameters	7358/1/378
Goodness-of-fit on F^2	1.053
Final R indexes [I>=2σ (I)]	R_1 = 0.0481, wR_2 = 0.1066
Final R indexes [all data]	R_1 = 0.0924, wR_2 = 0.1296
Largest diff. peak/hole / e Å^{-3}	0.44/-0.35

Table S6. Crystal data for Ti2b

Empirical formula	$C_{37}H_{48}Cl_2N_6O_2Ti$
Formula weight	727.61
Temperature/K	173.00
Crystal system	monoclinic
Space group	$P2_1/n$
a/Å	10.6343(7)
b/Å	30.9675(18)
c/Å	12.5823(8)
α/°	90
β/°	110.817(2)
γ/°	90
Volume/Å^3	3873.1(4)
Z	4
ρ_{calc}g/cm^3	1.248
μ/mm^{-1}	0.398
F(000)	1536.0
Crystal size/mm^3	0.1 × 0.025 × 0.025
Radiation	MoKα (λ = 0.71073)
2Θ range for data collection/°	4.304 to 61.016
Index ranges	-15 ≤ h ≤ 15, -44 ≤ k ≤ 44, -17 ≤ l ≤ 17
Reflections collected	150839
Independent reflections	11792 [R_{int} = 0.0482, R_{sigma} = 0.0239]
Data/restraints/parameters	11792/6/507
Goodness-of-fit on F^2	1.191
Final R indexes [I>=2σ (I)]	R_1 = 0.0600, wR_2 = 0.1306
Final R indexes [all data]	R_1 = 0.0700, wR_2 = 0.1352
Largest diff. peak/hole / e Å^{-3}	0.52/-0.53